Multi-omic rejuvenation of human cells by maturation phase transient reprogramming

Diljeet Gill[1], Aled Parry[1], Fátima Santos[1], Hanneke Okkenhaug[2], Christopher D Todd[1], Irene Hernando-Herraez[1], Thomas M. Stubbs[3], Inês Milagre[4,*] and Wolf Reik[1,5,6,7,*]

1. Epigenetics Programme, Babraham Institute, Cambridge, CB22 3AT, UK
2. Imaging Facility, Babraham Institute, Cambridge, CB22 3AT, UK
3. Chronomics Limited, 1 St James Court, Norwich, NR3 1RU, UK
4. Laboratory for Epigenetic Mechanisms/Chromosome Dynamics Lab, Instituto Gulbenkian de Ciência, Portugal
5. Altos Labs Cambridge Institute, Cambridge, CB21 6GP, UK
6. Wellcome Trust Sanger Institute, Hinxton, Cambridge, CB10 1SA, UK
7. Centre for Trophoblast Research, University of Cambridge, Cambridge, CB2 3EG, UK

*Correspondence: imilagre@igc.gulbenkian.pt (I.M.), wolf.reik@babraham.ac.uk (W.R.)

Abstract

Ageing is the gradual decline in organismal fitness that occurs over time leading to tissue dysfunction and disease. At the cellular level, ageing is associated with reduced function, altered gene expression and a perturbed epigenome. Somatic cell reprogramming, the process of converting somatic cells to induced pluripotent stem cells (iPSCs), can reverse these age-associated changes. However, during iPSC reprogramming, somatic cell identity is lost, and can be difficult to reacquire as re-differentiated iPSCs often resemble foetal rather than mature adult cells. Recent work has demonstrated that the epigenome is already rejuvenated by the maturation phase of reprogramming, which suggests full iPSC reprogramming is not required to reverse ageing of somatic cells. Here we have developed the first "maturation phase transient reprogramming" (MPTR) method, where reprogramming factors are expressed until this rejuvenation point followed by withdrawal of their induction. Using dermal fibroblasts from middle age donors, we found that cells temporarily lose and then reacquire their fibroblast identity during MPTR, possibly as a result of epigenetic memory at enhancers and/or persistent expression of some fibroblast genes. Excitingly, our method substantially rejuvenated multiple cellular attributes including the transcriptome, which was rejuvenated by around 30 years as measured by a novel transcriptome clock. The epigenome, including H3K9me3 histone methylation levels and the DNA methylation ageing clock, was rejuvenated to a similar extent. The magnitude of rejuvenation instigated by MTPR appears substantially greater than that achieved in previous transient reprogramming protocols. In addition, MPTR fibroblasts produced youthful levels of collagen proteins, and showed partial functional rejuvenation of their migration speed. Finally, our work suggests that more extensive reprogramming does not necessarily result in greater rejuvenation but instead that optimal time windows exist for rejuvenating the transcriptome and the epigenome. Overall, we demonstrate that it is possible to separate rejuvenation from complete pluripotency reprogramming, which should facilitate the discovery of novel anti-ageing genes and therapies.

Highlights

- We developed a novel method by which human fibroblasts are reprogrammed until the maturation phase of iPSCs and are then returned to fibroblast identity
- DNA methylation memory at fibroblast enhancers and persistent expression of certain fibroblast genes may allow recovery of cell identity when the majority of the fibroblast gene expression program is extinct
- Molecular measures of ageing including transcriptome, DNA methylation clocks and H3K9me3 levels reveal robust and substantial rejuvenation
- Functional rejuvenation of fibroblasts by MPTR is suggested by reacquisition of youthful levels of collagen proteins

Introduction

Ageing is the gradual decline in cell and tissue function over time that occurs in almost all organisms, and is associated with a variety of molecular hallmarks such as telomere attrition, genetic instability, epigenetic and transcriptional alterations and an accumulation of misfolded proteins[1]. This leads to perturbed nutrient sensing, mitochondrial dysfunction and increased incidence of cellular senescence, which impact overall cell function, intercellular communication, promotes exhaustion of stem cell pools and causes tissue dysfunction[1]. The progression of some ageing related changes, such as transcriptomic and epigenetic ones, can be measured highly accurately and as such they can be used to construct "ageing clocks" that predict chronological age with high precision in humans[2–5] and in other mammals[6–8]. Since transcriptomic and epigenetic changes are reversible at least in principle, this raises the intriguing question of whether molecular attributes of ageing can be reversed and cells phenotypically rejuvenated[9,10].

Induced pluripotent stem cell (iPSC) reprogramming is the process by which almost any somatic cell can be converted into an embryonic stem cell like state. Intriguingly, iPSC reprogramming reverses many age-associated changes including telomere attrition and oxidative stress[11]. Notably, the epigenetic clock is reset back to approximately 0, suggesting reprogramming can reverse ageing associated epigenetic alterations[3]. However, iPSC reprogramming also results in the loss of original cell identity and therefore function. By contrast, transient reprogramming approaches where the Yamanaka factors (Oct4, Sox2, Klf4, c-Myc) are expressed for short periods of time may be able to achieve rejuvenation without loss of cell identity. Reprogramming can be performed *in vivo*[12] and indeed, cyclical expression of the Yamanaka factors *in vivo* can extend lifespan in progeroid mice and improves cellular function in wild type mice[13]. An alternative approach for reprogramming *in vivo* also demonstrated reversal of ageing-associated changes in retinal ganglion cells and was capable of restoring vision in a glaucoma mouse model[14]. More recently, *in vitro* transient reprogramming has been shown to reverse multiple aspects of ageing in human fibroblasts and chondrocytes[15]. Nevertheless, the extent of epigenetic rejuvenation achieved by previous transient reprogramming methods has been modest (~3 years) compared to the drastic reduction achieved by complete iPSC reprogramming. A more detailed comparison of previous methods is provided in supplementary file 1. Here, we

establish a novel transient reprogramming strategy where Yamanaka factors are expressed until the maturation phase of reprogramming before abolishing their induction (maturation phase transient reprogramming, MPTR), with which we were able to achieve robust and very substantial rejuvenation (~30 years) whilst retaining original cell identity overall.

Results

Transiently reprogrammed cells reacquire their initial cell identity

Reprogramming can be divided into three phases: the initiation phase where somatic expression is repressed and a mesenchymal-to-epithelial transition occurs, the maturation phase, where a subset of pluripotency genes becomes expressed, and the stabilisation phase, where the complete pluripotency program is activated[16] (Figure 1A). Previous attempts at transient reprogramming have only reprogrammed within the initiation phase[13,15]. However, reprogramming further, up to the maturation phase, may achieve more substantial rejuvenation. To investigate the potential of maturation-phase transient reprogramming (MPTR) to reverse ageing phenotypes, we generated a doxycycline inducible polycistronic reprogramming cassette that encoded *Oct4, Sox2, Klf4, c-Myc* and GFP. By using a polycistronic cassette, we could ensure that individual cells were able to express all four Yamanaka factors. This reprogramming cassette was capable of generating iPSC lines from human fibroblasts and induced a substantial reduction of DNA methylation age throughout the reprogramming process, consistent with previous work using a different reprogramming system[17] (Figure 1A). Specifically, DNA methylation age as measured using the multi-tissue epigenetic clock[3] was substantially reduced relatively early in the reprogramming process (which takes about 50 days to complete in this system), with an approximate rejuvenation of 20 years by day 10 and 40 years by day 17 (Figure 1A). Similar results were obtained using the skin and blood clock[18] (Figure 1-figure supplement 1A). Interestingly, other epigenetic clocks were rejuvenated later in the reprogramming process. This may suggest that the epigenome is rejuvenated in stages, however, we note that these other epigenetic clocks were not trained on fibroblast data. We therefore focussed on the window between days 10 and 17 to develop our MPTR protocol for human fibroblasts (Figure 1B), predicting that this would enable substantial reversal of ageing phenotypes whilst potentially allowing cells to regain original cell identity. Beyond this window, cells would enter the stabilisation phase and the endogenous pluripotency genes would become activated, preventing the cessation of reprogramming by withdrawing doxycycline alone[16]. The reprogramming cassette was introduced into fibroblasts from three middle aged donors (chronologically aged 38, 53 and 53 years old and epigenetically aged 45, 49 and 55 years old, according to the multi-tissue epigenetic clock[3]) by lentiviral transduction before selecting successfully transduced cells by sorting for GFP. We then reprogrammed the fibroblasts for different lengths of time (10, 13, 15 or 17 days) by supplementing the media with 2 μg/mL doxycycline and carried out flow sorting to isolate cells that were successfully reprogramming (labelled “transient reprogramming intermediate”: SSEA4 positive, CD13 negative) as well as the cells that had failed to reprogram (labelled “failing to transiently reprogram intermediate”: CD13 positive, SSEA4 negative). At this stage, approximately 25% of the cells were successfully reprogramming and approximately 35% of the cells were failing to reprogram, whilst the remainder were double positive or double negative (Figure 1-figure supplement 1B). Cells were harvested for DNA methylation array or RNA-seq analysis and also re-plated for further culture in the absence of doxycycline to stop the expression of the reprogramming cassette. Further culture for a period of 4-5 weeks in the

absence of doxycycline generated “transiently reprogrammed fibroblasts”, which had previously expressed SSEA4 at the intermediate stage, as well as “failed to transiently reprogram fibroblasts”, which had expressed the reprogramming cassette (GFP-positive cells) but failed to express SSEA4. As a negative control, we simultaneously ‘mock infected’ (subject to transduction process but without lentiviruses) populations of fibroblasts from the same donors. These cells underwent an initial flow sort for viability (to account for the effects of the GFP sort) before culture under the same conditions as the reprogramming cells and flow sorting for CD13 (cells harvested at this stage generated a “negative control intermediate” for methylome and transcriptome analyses). Finally, these “negative control intermediate” cells were grown in the absence of doxycycline for the same length of time as experimental samples to account for the effects of extended cell culture, generating “negative control fibroblasts” (Figure 1B).

After reprogramming for 10-17 days, we found the fibroblasts had undergone dramatic changes in morphology. Upon visual inspection using a light microscope it appeared that the cells had undergone a mesenchymal to epithelial like transition and were forming colony structures that progressively became larger with longer periods of reprogramming, consistent with the emergence of the early pluripotency marker SSEA4. After sorting the cells and culturing in the absence of doxycycline, we found they were able to return to their initial fibroblast morphology, showing that morphological reversion is possible even after 17 days of reprogramming (Figure 1C). We quantified the morphology changes by calculating a ratio indicative of “roundness” (maximum length divided by perpendicular width) for individual cells before, during and after MPTR (Figure 1D and Figure 1-figure supplement 1C). We found that successfully reprogramming cells became significantly rounder at the intermediate stages of MPTR compared to the starting fibroblasts and then returned to an elongated state upon the completion of MPTR. Of note, we found that there was no significant difference in roundness between cells before and after MPTR, further supporting that fibroblasts were able to return to their original morphology. In comparison, failing to reprogram and negative control cells did not undergo as substantial a change during MPTR and were significantly more elongated at the intermediate stage (Supplementary file 2).

We investigated further the identity of the cells after MPTR by conducting DNA methylation array analysis and RNA sequencing to examine their methylomes and transcriptomes, respectively. We included published reprogramming datasets in our analysis as well as a novel reprogramming dataset that we generated based on Sendai virus delivery of the Yamanaka factors to act as a reference[5,19,20]. Principal component analysis using expression values of all genes in the transcriptome separated cells based on extent of reprogramming and the reference datasets formed a reprogramming trajectory along PC1 (Figure 1E). Transient reprogramming intermediate cells (collected after the reprogramming phase but before the reversion phase) clustered halfway along this trajectory, implying that cells lose aspects of the fibroblast transcriptional program and/or gain aspects of pluripotency transcriptional program, which is consistent with the loss of the fibroblast surface marker CD13 and gain of the iPSC surface marker SSEA4. We note that the different timepoints for the transient reprogramming intermediate samples clustered closer together when examining their transcriptomes compared to their DNA methylomes. This suggests that changes in the DNA methylome occur more gradually whereas changes in the transcriptome occur in more discrete stages. Notably upon completion of MPTR, transiently

reprogrammed samples clustered at the beginning of this trajectory showing that these samples once again transcriptionally resemble fibroblasts rather than reprogramming intermediates or iPSCs (Figure 1E). Similar findings were made when the reference datasets were excluded (Figure 1-figure supplement 1D). As examples, transiently reprogrammed cells did not express the pluripotency marker *NANOG* and expressed high levels of the fibroblast marker *FSP1* (Figure 1F). Notably, *NANOG* was temporarily expressed at high levels at the intermediate stages of transient reprogramming alongside FSP1, suggesting that these cells simultaneously possessed some transcriptional attributes of both fibroblasts and iPSCs.

Similarly, principal component analysis of the methylomes separated cells based on extent of reprogramming and the reference datasets formed a reprogramming trajectory along PC1. PC2 separated mid reprogramming samples from initial fibroblasts and final iPSCs and was driven by CpG sites that are temporarily hypermethylated or hypomethylated during reprogramming. These CpG sites appeared near genes associated with asymmetric protein localization according to gene ontology analysis. As with the transcriptome, intermediate samples from our transient reprogramming experiment clustered along this reprogramming trajectory (Figure 1G), showing that cells move epigenetically towards pluripotency. Notably, the transiently reprogrammed samples returned back to the start of this trajectory (with the reference fibroblast samples) revealing that they epigenetically resembled fibroblasts once again. Like the transcriptome, similar findings were made when the reference datasets were excluded (Figure 1-figure supplement 1E). We found typical regions that change during reprogramming were fibroblast-like after transient reprogramming[21], such as the promoter of *POU5F1* being hypermethylated and the promoter of *FSP1* being hypomethylated in our transiently reprogrammed cells (Figure 1H). Notably, the *POU5F1* promoter was temporarily demethylated and the *FSP1* promoter remained lowly methylated at the intermediate stages of transient reprogramming, suggesting that these intermediate stage cells possess some epigenetic features of both fibroblasts and iPSCs. Together, these data demonstrate that fibroblasts can be transiently reprogrammed to the maturation phase and then revert to a state that is morphologically, epigenetically and transcriptionally similar to the starting cell identity. To our knowledge, this is the first method for maturation phase transient reprogramming, where Yamanaka factors are transiently expressed up to the maturation phase of reprogramming before expression of the factors is abolished.

Epigenetic memory and transcriptional persistence are present at the intermediate stages of transient reprogramming

Though transiently reprogrammed fibroblasts temporarily lost their cell identity (becoming SSEA4 positive and CD13 negative) they were able to reacquire it once the reprogramming factors were removed, suggesting that they retained memory of their initial cell identity. To examine the source of this memory, we initially defined fibroblast-specific and iPSC-specific gene sets using differential expression analysis on fibroblasts before and after complete reprogramming with our system (Figure 2-figure supplement 1A). We subsequently analysed the expression of these gene sets throughout MPTR and observed that fibroblast-specific genes were temporarily downregulated whilst iPSC-specific genes were temporarily upregulated (Figure 2A). As expected, these gene sets were further downregulated and upregulated respectively during complete reprogramming (Figure 2A). We note that this

approach generalises the expression changes and as a result, may obscure subclusters within these gene sets that display different expression trajectories. Therefore, we analysed the expression levels of individual genes to gain further insight into these gene sets. After performing hierarchical clustering, we observed that the majority of genes within the fibroblast-specific gene set were temporarily downregulated during transient reprogramming (2803 genes out of 4178). However, we also observed that the remaining genes formed two additional clusters that were temporarily upregulated (961 genes) and persistently expressed (414 genes) respectively (Figure 2B, Figure 2-figure supplement 1B and Supplementary file 3). We also clustered the genes within the iPSC-specific gene set and observed that the majority of iPSC genes were upregulated in transient reprogramming intermediate cells to levels similar to iPSCs and the remaining genes were not yet activated (Figure 2-figure supplement 1C). We subsequently performed gene ontology analysis on the fibroblast-specific gene clusters and found that the temporarily upregulated cluster was enriched for gene ontology categories such as “response to lipopolysaccharide” suggesting that inflammatory signalling pathways are temporarily activated during transient reprogramming, likely in response to the reprogramming factors. Interestingly, the persistently expressed gene cluster was enriched for gene ontology categories such as extracellular matrix and collagen fibril organisation, suggesting that some aspects of fibroblast function are maintained during transient reprogramming at least at the transcriptional level (Figure 2-figure supplement 1D).

We also questioned whether the epigenome played a role in the retention of memory of the initial cell type, particularly for genes that were temporarily downregulated. We therefore examined the DNA methylation levels at regulatory elements linked to the fibroblast-specific genes. We used the Ensembl Regulatory Build[22] to obtain the locations of promoter and enhancer elements as well as their activity status in dermal fibroblasts and iPSCs. We then focussed on promoter and enhancer elements that are active in fibroblasts and linked them to the nearest transcription start site (within 1kb for promoters and 1mb for enhancers). The promoters associated with fibroblast genes remained lowly methylated throughout transient reprogramming and complete reprogramming regardless of the gene cluster, suggesting that promoter methylation does not contribute substantially towards memory (Figure 2-figure supplement 1E). In contrast, enhancers associated with fibroblast genes gained DNA methylation but only during complete reprogramming and not during transient reprogramming (Figure 2C and Figure 2-figure supplement 1F). This was the case for enhancers linked to the genes in all three clusters and in the case of temporarily downregulated genes, the lack of hypermethylation may confer epigenetic memory at a time when the associated genes are transcriptionally repressed. We also examined fibroblast-specific enhancers in general and defined these as enhancers that are active in fibroblasts but are no longer active in iPSCs. Similar to the previous analysis, we found that DNA methylation was relatively dynamic at fibroblast-specific enhancers. Approximately half of all fibroblast-specific enhancers (2351 out of the covered 4204 enhancers) gained DNA methylation during iPSC reprogramming. However, even at day 17 of the reprogramming process (the longest transient reprogramming intermediate tested here), these enhancers still remained hypomethylated (Figure 2D). Overall, we hypothesise that both epigenetic memory at genes such as MMP1 (Figure 2E) and transcriptional persistence at genes such as COL1A2 (Figure 2E) enable cells to return to their original cell type once the reprogramming factors are withdrawn. Together, these two attributes may act as the source of memory for

initial cell identity during a time when the somatic transcriptional program is otherwise mostly repressed and somatic proteins such as CD13 are lost[23,24].

Transient reprogramming reverses age-associated changes in the transcriptome and partially restores fibroblast function

We next investigated the transcriptome to determine if there was any evidence of rejuvenation in this omic layer. We initially identified genes that significantly correlated with age in a reference fibroblast ageing dataset[5] and used genes with a significant Pearson correlation after Bonferroni correction ($P \leq 0.05$) to carry out principal component analysis (3707 genes). The samples primarily separated by age and reference fibroblast samples formed an ageing trajectory. The transiently reprogrammed samples clustered closer to the young fibroblasts along PC1 than the negative control samples (Figure 3A). Based on the relationship between PC1 and age in the reference dataset, we inferred that transient reprogrammed samples were approximately 40 years younger than the negative control samples (Figure 3B). To further quantify the extent of rejuvenation, we investigated the effect of MPTR using transcription clocks. Unfortunately, existing transcription clocks failed to accurately predict the age of our negative control samples. This may be due to batch effects such as differences in RNA-seq library preparation and data processing pipelines. To overcome this problem, we trained a transcription age-predictor using random forest regression on published fibroblast RNA-seq data from donors aged 1-94 years old that was batch corrected to our transient reprogramming dataset[5]. The transcription age predictor was trained on transformed age, similar to the Horvath epigenetic clock, to account for the accelerated ageing rate during childhood and adolescence[3]. The final transcription age predictor had a median absolute error of 12.57 years (Figure 3-figure supplement 1A), this error being higher than that of the epigenetic clock consistent with previous transcription age predictors[4,5]. Using our predictor, we found that transient reprogramming reduced mean transcription age by approximately 30 years (Figure 3C). We also observed a moderate reduction in transcription age in cells that failed to transiently reprogram (SSEA4 negative at the intermediate timepoint), suggesting expression of the reprogramming factors alone was capable of rejuvenating some aspects of the transcriptome. Interestingly, we observed that MPTR with longer reprogramming phases reduced the extent of rejuvenation, suggesting that 10 or 13 days may be the optimum for transcriptional rejuvenation. We note that the reduction in transcription age from MPTR appears to be greater than that recently achieved by transient transfection of the Yamanaka factors[15], which was by approximately 10 years according to our transcription age predictor (Figure 3-figure supplement 1B), consistent with our approach of reprogramming further into the maturation phase rather than only up to the end of the initiation phase. Recently, a novel transcription clock called BiT age clock has been defined[25], which has been trained on binarized gene expression levels. This clock has a very low median absolute error, which is comparable to that of epigenetic clocks. We ran a retrained version of the BiT age clock on our dataset and made similar findings to our random forest-based clock. Of note, we observed that transient reprogramming also rejuvenated the BiT age clock by approximately 20 years relative to negative controls and that 10 or 13 days of reprogramming was optimal for maximal transcriptional rejuvenation (Figure 3-figure supplement 1C).

We further profiled the effects of MPTR with 13 days of reprogramming (due to its apparent significance) by examining the whole transcriptome. This was achieved by comparing the

expression levels of genes in transiently reprogrammed cells to those in negative control cells and subsequently overlaying the expression change due to age calculated using the reference ageing dataset[5]. As expected, we observed an overall reversal of the ageing trends, with genes upregulated during ageing being downregulated following transient reprogramming and genes downregulated during ageing being upregulated following transient reprogramming (Figure 3D, Figure 3-figure supplement 1D). Notably, structural proteins downregulated with age that were upregulated upon transient reprogramming included the cytokeratins 8 and 18 as well as subunits of collagen IV.

The production of collagens is a major function of fibroblasts[26], thus we examined the expression of all collagen genes during fibroblast ageing and after transient reprogramming with 13 days of reprogramming (Figure 3E). As shown previously[27,28], we found collagen I and IV were downregulated with age, with collagen IV demonstrating a more dramatic reduction. Notably the expression of both genes was restored to youthful levels after transient reprogramming, though this was not significant for collagen I likely due to the small expression difference associated with age and lower number of samples (Figure 3E). We then assessed by immunofluorescence whether this increased mRNA expression resulted in increased protein levels and indeed found that transient reprogramming resulted in an increase in Collagen I and IV protein towards more youthful levels (Figure 3F). Fibroblasts are also involved in wound healing responses[29], so we investigated the impact of transient reprogramming on this function using an *in vitro* wound healing assay (Figure 3G and Figure 3-figure supplement 1E). We found that migration speed was significantly reduced in our control fibroblasts from middle-aged donors compared to fibroblasts from young donors (aged 20-22 years old). Transient reprogramming improved the median migration speed, however, the individual responses were quite variable and in some cases migration speed was improved and in other cases it was unaffected. Interestingly, this did not appear to correlate with other ageing measures such as transcription and methylation clocks. Our data show that transient reprogramming followed by reversion can rejuvenate fibroblasts both transcriptionally and at the protein level, at least based on collagen production, and functionally at least in part. This indicates that our rejuvenation protocol can, in principle, restore youthful functionality in human cells.

Optimal transient reprogramming reverses age-associated changes in the epigenome

After finding evidence of transcriptomic rejuvenation, we sought to determine whether there were also aspects of rejuvenation in the epigenome. We initially examined global levels of H3K9me3 by immunofluorescence. H3K9me3 is a histone modification associated with heterochromatin that has been previously shown to be reduced globally with age in a number of organisms[30], including in human fibroblasts[31,32]. We were able to confirm this observation and found that MPTR was able to substantially reverse this age-associated reduction back to a level comparable with fibroblasts from younger donors (with a mean age of 33 years old). Both 10 and 13 days of transient reprogramming increased global levels of H3K9me3 suggesting that this epigenetic mark, similar to the transcriptome, has a relatively broad window for rejuvenation by transient reprogramming. We also observed a slight increase in H3K9me3 levels in cells that failed to transiently reprogram, suggesting that expression of the reprogramming factors alone is capable of partially restoring this epigenetic mark (Figure 4A), as was observed for our transcriptome-based age-predictor

(Figure 3C). The magnitude of rejuvenation in H3K9me3 levels in our transiently reprogrammed cells is similar to that observed from initiation phase transient reprogramming[15].

We next applied the epigenetic clock, a multi-tissue age predictor that predicts age based on the DNA methylation levels at 353 CpG sites[3], to our data. Notably, with 13 days of transient reprogramming we observed a substantial reduction of the median DNA methylation age – by approximately 30 years, quantitatively the same rejuvenation as we saw in the transcriptome (Figure 4B). A shorter period of transient reprogramming (10 days) resulted in a smaller reduction of DNA methylation age, consistent with our results profiling DNA methylation age throughout the reprogramming process, where DNA methylation age gradually reduced throughout the maturation phase (Figure 1A). This epigenetic rejuvenation is potentially promoted by *de novo* methylation and active demethylation as the *de novo* methyltransferases and TET enzymes are upregulated during the maturation phase (Figure 4-figure supplement 1A). Potentially, some of the rejuvenating mechanisms occurring in MPTR may mirror those that occur during embryonic development as epigenetic rejuvenation during embryonic development coincides with *de novo* methylation of the genome[33]. Similar to the transcription clocks, we also observed a smaller reduction in DNA methylation age with longer transient reprogramming times, suggesting that some aspects of the observed epigenetic rejuvenation are lost during the reversion phase of our MPTR protocol. Potentially, extended reprogramming (for 15 or 17 days) may make reversion more difficult and result in cellular stresses that 're-age' the methylome during the process. Similar results were obtained using the skin and blood clock and the Weidner clock[18,34] (Figure 4-figure supplement 1B). Other epigenetic clocks were not rejuvenated by maturation phase transient reprogramming, however, we note that these clocks either rejuvenate later in the reprogramming process or are unaffected by reprogramming (Figure 1-figure supplement 1A).

Telomeres are protective structures at the ends of chromosomes that consist of repetitive sequences. Telomere length decreases with age due to cell proliferation in the absence of telomerase enzymes and is restored upon complete iPSC reprogramming[11]. To investigate the effect of transient reprogramming on telomere length, we used the telomere length clock, which predicts telomere length based on the methylation levels at 140 CpG sites[35]. We found that MPTR does not affect telomere length and, in some cases, slightly reduces it (Figure 4C). This is consistent with our results profiling telomere length throughout complete reprogramming using our doxycycline inducible system, where telomere length did not increase until the stabilisation phase (Figure 4-figure supplement 1C). This coincides with the expression of telomerase during reprogramming, where it is weakly expressed during the later stages of the maturation phase and only strongly expressed during the stabilisation phase (Figure 4-figure supplement 1D).

Next, we investigated the locations of the rejuvenated CpG sites and found that most were individual sites spread across the genome (Figure 4-figure supplement 1E). Some of these individual CpG sites may be part of larger regions of rejuvenated methylation, which we are unable to fully detect due to the targeted nature of DNA methylation array profiling, however, we found a few small clusters of rejuvenated CpG sites. We found that a small region in the *IRX5* promoter became demethylated with age and transient reprogramming

was able to partially remethylate this region (Figure 4D). IRX5 is involved in embryonic development so demethylation of its promoter with age may lead to inappropriate expression[36,37]. We also found two regions that became hypermethylated with age and were demethylated by transient reprogramming (Figure 4E). One of these regions is in the *GAD1* promoter; encoding an enzyme that catalyses the conversion of gamma-aminobutyric acid into glutamic acid[38]. The other region is within the *HOXB* locus, involved in anterior-posterior patterning during development[39]. Finally, we examined whether there was any overlap between the epigenetic and transcriptional rejuvenation. We therefore annotated the rejuvenated CpG sites with the nearest gene and then overlapped this gene set with the list of genes with rejuvenated expression. We found that there was a significant overlap between these two groups suggesting that epigenetic rejuvenation and transcriptional rejuvenation may be partially linked (Figure 4F). We further examined these overlapping genes and found that several had structural roles. These included *FBN2* and *TNXB*, which encode components of the extracellular matrix[40,41] and *SPTB*, which encodes a component of the cytoskeletal network[42]. WISP2 was also rejuvenated transcriptionally and epigenetically; this gene is an activator of the canonical WNT pathway[43] and has recently been shown to inhibit collagen linearisation[44]. ASPA and STRA6 respectively encode an enzyme that hydrolyses N-acetyl-I-aspartate and a vitamin A receptor[45,46]. Neither of these genes have obvious roles in fibroblasts. We note that additional overlaps between epigenetic and transcriptional rejuvenation may exist that are not observed in our study due to the limited genomic coverage of DNA methylation arrays. Overall, our data demonstrate that transient reprogramming for 13 days (but apparently not for longer or shorter periods) represents a 'sweet spot' that facilitates partial rejuvenation of both the methylome and transcriptome, reducing epigenetic and transcriptional age by approximately 30 years.

Discussion

Here we have developed a novel method, maturation phase transient reprogramming (MPTR), where the Yamanaka factors are ectopically expressed until the maturation phase of reprogramming is reached, and their induction is then withdrawn. MPTR rejuvenates multiple molecular hallmarks of ageing robustly and substantially, including the transcriptome, epigenome, functional protein expression, and cell migration speed. Previous attempts at transient reprogramming have been restricted to the initiation phase in order to conserve initial cell identity[13–15]. This is a valid concern as fully reprogrammed iPSCs can be difficult to differentiate into mature adult cells and instead these differentiated cells often resemble their foetal counterparts[47]. With our approach, cells temporarily lose their identity as they enter the maturation phase but, importantly, reacquire their initial somatic fate when the reprogramming factors are withdrawn. This may be the result of persisting epigenetic memory at enhancers[48], which notably we find is not erased until the stabilisation phase, as well as persistent expression of some fibroblast genes.

With our method employing longer periods of reprogramming, we observed robust and substantial rejuvenation of the whole transcriptome as well as aspects of the epigenome, with many features becoming approximately 30 years younger. This extent of rejuvenation appears to be substantially greater than what has been observed previously for transient reprogramming approaches that reprogram within the initiation phase. The methylome appears to require longer reprogramming to substantially rejuvenate and consequently,

previous work using shorter lengths of reprogramming resulted in modest amounts of rejuvenation of the methylome[14,15]. However, we note that future studies are required to thoroughly compare these approaches with our method, ideally being performed in parallel on the same starting material and with the same reprogramming system, especially as different reprogramming systems can reprogram cells at different speeds[49]. Interestingly, these findings demonstrate that different parts of the epigenome undergo contrasting changes during transient reprogramming with age-associated CpG sites becoming differentially methylated during the maturation phase and cell-identity regions remaining unchanged until the stabilisation phase. The CpG sites within these two categories are distinct and the differential timing may suggest that different and potentially specific mechanisms are responsible for these changes. Telomere attrition is another ageing hallmark, which can induce DNA damage and senescence[1]. Consistent with previous studies[50], our reprogramming system did not induce telomere elongation until the stabilisation phase, likely explaining why telomeres were not elongated by MPTR.

More recently, there have been *in vivo* transient reprogramming approaches that elicit similar magnitudes of rejuvenation to our *in vitro* MPTR method. In mice, one week of reprogramming induction followed by 2 weeks of recovery reversed age-associated expression changes (including collagen gene expression) and partially rejuvenated the DNA methylome in the pancreas[51]. Interestingly, these outcomes closely mirror those observed in our human fibroblasts after MPTR. We note that iPSC reprogramming proceeds faster in mouse cells than human cells[52] and so this *in vivo* approach likely also reprograms up to the maturation phase, supporting our findings that transient reprogramming up to the maturation phase can substantially reverse multiple features of ageing. In another recent approach, reprogramming was cyclically induced in mice for 2 days followed by 5 days of recovery for 7 months. This substantially reversed epigenetic clocks by up to 0.4 years (equivalent to 20 years in humans, similar to our system)[53]. These results suggest that the rejuvenation from shorter periods of transient reprogramming is additive and when performed long-term can reach the magnitude elicited by MPTR.

Quantifying the age of the transcriptome is challenging and our attempts to quantify transcriptional rejuvenation suggested varying magnitudes ranging from 20 to 40 years. In addition, we needed to apply batch correction to compare to reference ageing datasets. There is a need in the field for a more robust transcription clock that can predict age accurately and can be applied to other datasets without the need to batch correct. Such a tool would be invaluable and enable us to quantify more accurately the true extent of transcriptional rejuvenation arising from MPTR.

Upon further interrogation of the transcriptomic rejuvenation, we also observed changes in genes with non-fibroblast functions. In particular, the age-associated downregulation of *APBA2* and the age-associated upregulation of *MAF* were reversed (Figure 3D). APBA2 stabilises amyloid precursor protein, which plays a key role in the development of Alzheimer's disease[54]. MAF regulates the development of embryonic lens fibre cells, and defects in this gene lead to the development of cataracts, which are a frequent complication in older age[55]. These observations may signal the potential of MPTR to promote more general rejuvenation signatures that could be relevant for other cell types such as neurons. It will be interesting to determine if MPTR-induced rejuvenation is possible in other cell

types, which could help us understand and potentially treat age-related diseases such as Alzheimer's disease and cataracts. Potentially we may be able to rejuvenate *ex vivo* clinically relevant cell types and administer these rejuvenated cells as an autologous cell therapy, for example fibroblasts rejuvenated by MPTR may be applicable for treating skin wounds and improve wound healing. In addition, we may be able to use MPTR as a screening platform to find novel candidate genes that are responsible for reversing age-associated changes during reprogramming. Potentially by targeting such genes, we may be able to reverse age-associated changes without inducing pluripotency.

In our study, we investigated different lengths of reprogramming for our MPTR method and surprisingly found that longer lengths of reprogramming did not always promote more rejuvenation in the transcriptome and epigenome. Instead, we found that 13 days of reprogramming was the optimal period and that longer lengths of reprogramming diminished the extent of transcriptional and epigenetic rejuvenation. This finding contrasts with the observations of cells undergoing complete iPSC reprogramming and highlights the importance of assessing multiple reprogramming durations when using transient reprogramming approaches.

The Yamanaka factors possess oncogenic properties, which can lead to teratoma formation when persistently overexpressed *in vivo*[12,56]. Our approach should avoid these properties as we only temporarily express the factors, similar to other transient reprogramming approaches[13,15]. Whilst we could not find any signatures of pluripotency within the transcriptomes or methylomes of transiently reprogrammed cells, we cannot discount the possibility that a minor subset of cells within the population maintain pluripotent-like characteristics, and could therefore induce teratoma formation if transplanted *in vivo*. We note though that this is a proof-of-concept study and that the method will eventually require modifications to be more suitable for therapeutic applications, such as by replacing the lentiviral vectors with non-integrating vectors.

The effect of starting age is a factor that remains to be explored. In our study, we examined the effects of MPTR on fibroblasts from middle-aged donors and observed an approximately 30 year rejuvenation. It will be interesting to perform our method on fibroblasts from younger and older donors to see if the rejuvenating effect of MPTR is constant in that case cells would always become 30 years younger than their controls. Alternatively, the effect of MPTR may scale with starting age, with more rejuvenation being observed in cells from older donors compared to cells from younger donors. Finally, we note that multiple cycles of transient reprogramming can be performed with some approaches[13]. It will be interesting to examine if MPTR can be performed repeatedly on cells and if this may improve the extent of rejuvenation. However, this may not be possible with our current system as telomere length is unaffected by MPTR. In addition, multiple cycles may not improve the extent of rejuvenation as there may be a minimum age that can be achieved when limiting reprogramming to the maturation phase.

Overall, our results demonstrate that substantial rejuvenation is possible without acquiring stable pluripotency and suggest the exciting concept that the rejuvenation program may be separable from the pluripotency program. Future studies are warranted to determine the

extent to which these two programs can be separated and could lead to discovery of novel targets that promote rejuvenation without the need for iPSC reprogramming.

Methods

Plasmids and lentivirus production

The doxycycline inducible polycistronic reprogramming vector was generated by cloning a GFP-IRES sequence downstream of the tetracycline response element in the backbone FUW-tetO-hOKMS (Addgene 51543, a gift from Tarjei Mikkelsen[57]). This vector was used in combination with FUW-M2rtTA (Addgene 20342, a gift from Rudolf Jaenisch[58]). Viral particles were generated by transfecting HEK293T cells with the packaging plasmids pMD2.G (Addgene 12259, a gift from Didier Trono) and psPAX2 (Addgene 12260, a gift from Didier Trono) and either FUW-tetO-GFP-hOKMS or FUW-M2rtTA.

iPSC reprogramming

Dermal fibroblasts from middle age donors (38-53 years old) were purchased from Lonza and Gibco and were used at passage 4 after purchase for reprogramming experiments. Cells were routinely tested for mycoplasma. For lentiviral iPSC reprogramming, fibroblasts were expanded in fibroblast medium (DMEM-F12, 10% FBS, 1X Glutamax, 1X MEM-NEAA, 1X beta-mercaptoethanol, 0.2X Penicillin/Streptomycin, 16 ng/ml FGF2) before being spinfected with tetO-GFP-hOKMS and M2rtTA lentiviruses, where 10% virus supernatant and 8 µg/ml polybrene was added to the cells before centrifugation at 1000 rpm for 60 minutes at 32°C. Reprogramming was initiated 24 hours after lentiviral transduction by introducing doxycycline (2 µg/ml) to the media. Media was changed daily throughout the experiment subsequently. On day 2 of reprogramming, cells were flow sorted for viable GFP positive cells and then cultured on gelatine coated plates. On day 7 of reprogramming, cells were replated onto irradiated mouse embryonic fibroblasts (iMEFs) and on day 8 of reprogramming, the medium was switched to hES medium (DMEM-F12, 20% KSR, 1X Glutamax, 1X MEM-NEAA, 1X beta-mercaptoethanol, 0.2X Penicillin/Streptomycin, 8 ng/ml FGF2). For transient reprogramming, cells were flow sorted at day 10, 13, 15 or 17 of reprogramming for the CD13+ SSEA4- and CD13- SSEA4+ populations. These cells were then replated on iMEFs (to replicate culture conditions before the flow sort and aid in cell reattachment) in fibroblast medium without doxycycline and then maintained like fibroblasts without iMEFs for subsequent passages. Cells were grown without doxycycline for 4 weeks in the first experiment and 5 weeks in the second experiment. Cells had returned to fibroblast morphology by four weeks in the second experiment, however, needed to be further expanded to generate enough material for downstream analyses. Negative control cells underwent the same procedure as the transient reprogramming cells to account for the effects of growing cells on iMEFs in hES media, flow sorting cells and keeping cells in culture for extensive periods of time. These confounders appeared to have no major effects on fibroblasts as these cells still clustered with the starting fibroblasts in our principal component analyses (Figure 1-figure supplement 1D and 1E). For complete reprogramming, colonies were picked on day 30 of reprogramming and transferred onto Vitronectin coated plates in E8 medium without doxycycline. Colonies were maintained as previously described [59] and harvested at day 51 of reprogramming to ensure that the stabilisation phase was completed and that traces of donor memory were erased. For Sendai virus iPSC reprogramming using CytoTune™-iPS 2.0 Sendai Reprogramming kit

(Invitrogen), fibroblasts were reprogrammed as previously described[59]. For intermediate timepoints, cells were flow sorted into reprogramming (CD13- SSEA4+) and not reprogramming populations (CD13+ SSEA4-) before downstream profiling.

Fluorescence-activated cell sorting (FACS) of reprogramming intermediates

Cells were pre-treated with 10 µM Y-27632 (STEMCELL technologies) for 1 hour. Cells were harvested using StemPro™ Accutase™ cell dissociation reagent and incubated with antibodies against CD13 (PE, 301704, Biolegend), SSEA4 (AF647, 330408, Biolegend) and CD90.2 (APC-Cy7, 105328, Biolegend) for 30 minutes. Cells were washed twice with 2% FBS in PBS and passed through a 50 µm filter to achieve a single cell suspension. Cells were stained with 1 µg/mL DAPI just prior to sorting. Single colour controls were used to perform compensation and gates were set based on the "negative control intermediate" samples. Cells were sorted with a BD FACSAria™ Fusion flow cytometer (BD Biosciences) and collected for either further culture or DNA/RNA extraction.

DNA methylation array

Genomic DNA was extracted from cell samples with the DNeasy blood and tissue kit (Qiagen) by following the manufacturer's instructions and including the optional RNase digestion step. For intermediate reprogramming stage samples, genomic DNA was extracted alongside the RNA with the AllPrep DNA/RNA mini kit (Qiagen). Genomic DNA samples were processed further at the Barts and the London Genome Centre and run on Infinium MethylationEPIC arrays (Illumina).

RNA-Seq

RNA was extracted from cell samples with the RNeasy mini kit (Qiagen) by following the manufacturer's instructions. For intermediate reprogramming stage samples and Sendai virus reprogrammed samples, RNA was extracted alongside the genomic DNA with the AllPrep DNA/RNA mini kit (Qiagen). RNA samples were DNase treated (Thermo Scientific) to remove contaminating DNA. RNA-Seq libraries were prepared at the Wellcome Sanger Institute and run on a HiSeq 2500 system (Illumina) for 50 bp single-end sequencing. For Sendai virus reprogrammed samples, libraries were prepared as previously described[59], and run on a HiSeq 2500 (Illumina) for 75 bp paired-end sequencing.

DNA methylation analysis

The array data was processed with the minfi R package and NOOB normalisation to generate beta values. DNA methylation age was calculated using the multi-tissue clock[3], the skin and blood clock[18], the epiTOC clock[60], the GrimAge clock[61], the Hannum clock [2], the PhenoAge [62] and the Weidner clock [34]. We note that 19 CpG sites from the multi-tissue clock are missing in the Infinium MethylationEPIC array, however, the predictions are still robust when performed on NOOB normalised array data[63]. Telomere length was calculated using the telomere length clock[35]. Reference datasets for reprogramming fibroblasts and iPSCs were obtained from Ohnuki et al[19] (GEO: GSE54848), Banovich et al[20] (GEO: GSE110544) and Horvath et al[18]. In addition, the reference datasets included novel data examining the intermediate stages of dermal fibroblasts being reprogrammed with the CytoTune™-iPS 2.0 Sendai Reprogramming kit (Invitrogen).

RNA-Seq analysis

Reads were trimmed with Trim Galore (version 0.6.2) and aligned to the human genome (GRCh38) with Hisat2 (version 2.1.0). Raw counts and log2 transformed counts were generated with Seqmonk (version 1.45.4). Reference datasets for fibroblasts and iPSCs were obtained from Fleischer et al[5] (GEO: GSE113957) and Banovich et al[20] (GEO: GSE107654). In addition, the reference datasets included novel data examining the intermediate stages of dermal fibroblasts being reprogrammed with the CytoTune™-iPS 2.0 Sendai Reprogramming kit (Invitrogen). Samples were carried forward for further analysis if they had a total read count of at least 500000 with at least 70% of the reads mapping to genes and at least 65% of the reads mapping to exons.

Immunofluorescence and Imaging

Young control dermal fibroblasts were purchased from Lonza, Gibco and the Coriell Institute (GM04505, GM04506, GM07525, GM07545 and AG09309) and were used at passage 4 after purchase. Antibody staining was performed as previously described[64] on cells grown on coverslips or cytospun onto coverslip after fixation with 2% PFA for 30 minutes at room temperature. Briefly, cells were permeabilised with 0.5% TritonX-100 in PBS for 1 hour; blocked with 1% BSA in 0.05% Tween20 in PBS (BS) for 1 hour; incubated overnight at 4°C with the appropriate primary antibody diluted in BS; followed by wash in BS and secondary antibody. All secondary antibodies were Alexa Fluor conjugated (Molecular Probes) diluted 1:1000 in BS and incubated for 30 minutes. For the morphology analysis, cells were not permeabilised and were stained with direct labelled primary antibodies. Incubations were performed at room temperature, except where stated otherwise. DNA was counterstained with 5 µg/mL DAPI in PBS. Optical sections were captured with a Zeiss LSM780 microscope (63x oil-immersion objective). Fluorescence semi-quantification analysis was performed with Volocity 6.3 (Improvision). 3D rendering of z-stacks was used for semi-quantification of Collagen I and IV. Single middle optical sections were used for semi-quantification of H3K9me3. Antibodies and dilutions used are listed below:

Anti-H3K9me3; 07-442, Merck/ Millipore (1:500)
Anti-Collagen I; ab254113, Abcam (1:400)
Anti-Collagen IV; PA5-104508, Invitrogen (1:200)
Anti-CD44-BB515; 564587, BD Biosciences (1:400)
Anti-SSEA4-APC; FAB1435A-100; R&D Systems (1:40)
Anti-CD13-PE; 301704; Biolegend (1:500)

Wound healing assay

Cells were seeded into wound healing assay dish (80466, Ibidi) at a cell density of 20000 cells per chamber. GM04505, GM04506, GM07545 and AG09309 fibroblasts were used at passage 5 as young controls. After 24 hours, the insert was removed generating 500 µm gaps between the cell-containing areas. The dishes were imaged every 20 minutes for 20 hours using a Nikon Ti-E equipped with a full enclosure incubation chamber (37^{o} C; 5% CO_2) and the 20x objective. The images were pre-processed by cropping and rotating so that the wound area was on the right-hand side of the image. A Fiji macro was used to generate masks of the wound healing images. The coverage of the wound by immerging cells was analysed by measuring the intensity of the mask along a line across the image. R was used

to determine the location of the wound edge by collecting all of the x coordinates where the mask intensity was high enough to indicate that it was no longer part of the wound. The wound edge at each timepoint was expressed relative to the starting position to obtain the distance closed. Migration speed was calculated from the gradient between distance closed and time.

Data analyses

Downstream analyses of RNA-seq and DNA methylation data were performed using R (version 4.0.2). Ggplot2 (version 3.3.2) was used to generate the bar charts, boxplots, line plots, pie charts, scatter plots and violin plots. Ggalluvial (version 0.12.2) was used to generate the alluvial plots. ComplexHeatmap (version 2.4.3) was used to generate the heatmaps. The combat function from the package sva (version 3.36.0) was used in figures 1E and 1F to batch correct the novel Sendai reprogramming dataset to the other datasets. The combat function was also used in figure 3 to batch correct the fibroblast ageing reference dataset[5] to our dataset. Non-parametric tests were used when the data distribution was not normal and parametric tests were used when the data distribution was normal.

The random forest-based transcription clock was trained on the batch corrected ageing reference dataset using the caret R package[65] and random forest regression with 10-fold cross validation, 3 repeats and a "tuneLength" of 5. Chronological age was transformed before training with the following formulas adapted from the Horvath multi-tissue epigenetic clock[3]:

$F(age)=\log_2(chronological.age+1)-\log_2(adult.age+1)$ if $chronological.age<=adult.age$

$F(age)=(chronological.age-adult.age)/(adult.age+1)$ if $chronological.age>adult.age$

As with the Horvath multi-tissue epigenetic clock, adult.age was set to 20 years old for these calculations[3]. The BiT age clock was also retrained on the batch corrected ageing reference dataset using scikit-learn as previously described[25]. This retrained model had a median absolute error of 5.55 years and consisted of 29 genes.

Rejuvenated CpG sites were found by comparing the methylation difference due to the age (calculated with the Horvath et al, 2018 dataset) to the methylation difference due to 13 days of transient reprogramming. CpG sites were classified as rejuvenated if they demonstrated a methylation difference of 10% over 40 years of ageing that was reversed by transient reprogramming.

Data availability

DNA methylation array and RNA-seq data are available on Gene Expression Omnibus under the accession number: GSE165180. For the purposes of reviewing, data is available with the token: mvivgksmxjcdjwf

Acknowledgements

We would like to thank all members of the Reik lab for helpful discussions. We would like to thank the bioinformatics facility at the Babraham Institute for processing the sequencing

data, and the flow cytometry facility at the Babraham Institute for cell sorting. We would also like to thank the sequencing facilities at the Sanger Institute and the Bart's and the London Genome Centre for sequencing and methylation array services respectively. This work was funded by the BBSRC. A.P. is supported by a Sir Henry Wellcome Fellowship (215912/Z/19/Z). W.R. is a consultant and shareholder of Cambridge Epigenetix. T.S. is CEO and shareholder of Chronomics.

References

1. López-Otín, C., Blasco, M. A., Partridge, L., Serrano, M. & Kroemer, G. The hallmarks of aging. *Cell* **153**, 1194–1217 (2013).
2. Hannum, G. *et al.* Genome-wide methylation profiles reveal quantitative views of human aging rates. *Mol. Cell* **49**, 359–367 (2013).
3. Horvath, S. DNA methylation age of human tissues and cell types. *Genome Biol.* **14**, R115 (2013).
4. Peters, M. J. *et al.* The transcriptional landscape of age in human peripheral blood. *Nat. Commun.* **6**, 8570 (2015).
5. Fleischer, J. G. *et al.* Predicting age from the transcriptome of human dermal fibroblasts. *Genome Biol.* **19**, 221 (2018).
6. Stubbs, T. M. *et al.* Multi-tissue DNA methylation age predictor in mouse. *Genome Biol.* **18**, 68 (2017).
7. Thompson, M. J., von Holdt, B., Horvath, S. & Pellegrini, M. An epigenetic aging clock for dogs and wolves. *Aging (Albany. NY).* **9**, 1055–1068 (2017).
8. Thompson, M. J. *et al.* A multi-tissue full lifespan epigenetic clock for mice. *Aging (Albany. NY).* **10**, 2832–2854 (2018).
9. Rando, T. A. & Chang, H. Y. Aging, rejuvenation, and epigenetic reprogramming: Resetting the aging clock. *Cell* **148**, 46–57 (2012).
10. Manukyan, M. & Singh, P. B. Epigenetic rejuvenation. *Genes to Cells* **17**, 337–343 (2012).
11. Lapasset, L. *et al.* Rejuvenating senescent and centenarian human cells by reprogramming through the pluripotent state. *Genes Dev.* **25**, 2248–2253 (2011).
12. Abad, M. *et al.* Reprogramming in vivo produces teratomas and iPS cells with totipotency features. *Nature* **502**, 340–345 (2013).
13. Ocampo, A. *et al.* In Vivo Amelioration of Age-Associated Hallmarks by Partial Reprogramming. *Cell* **167**, 1719-1733.e12 (2016).
14. Lu, Y. *et al.* Reprogramming to recover youthful epigenetic information and restore vision. *Nature* **588**, 124–129 (2020).
15. Sarkar, T. J. *et al.* Transient non-integrative expression of nuclear reprogramming factors promotes multifaceted amelioration of aging in human cells. *Nat. Commun.* **11**, 1–12 (2020).
16. Samavarchi-Tehrani, P. *et al.* Functional genomics reveals a BMP-Driven mesenchymal-to-Epithelial transition in the initiation of somatic cell reprogramming. *Cell Stem Cell* **7**, 64–77 (2010).
17. Olova, N., Simpson, D. J., Marioni, R. & Chandra, T. Partial reprogramming induces a steady decline in epigenetic age before loss of somatic identity. *bioRxiv* (2018).
18. Horvath, S. *et al.* Epigenetic clock for skin and blood cells applied to Hutchinson Gilford Progeria Syndrome and ex vivo studies. *Aging (Albany. NY).* **10**, 1758–1775

(2018).
19. Ohnuki, M. *et al.* Dynamic regulation of human endogenous retroviruses mediates factor-induced reprogramming and differentiation potential. *Proc. Natl. Acad. Sci.* **111**, 12426–12431 (2014).
20. Banovich, N. E. *et al.* Impact of regulatory variation across human iPSCs and differentiated cells. *Genome Res.* **28**, 122–131 (2018).
21. Takahashi, K. *et al.* Induction of Pluripotent Stem Cells from Adult Human Fibroblasts by Defined Factors. *Cell* **131**, 861–872 (2007).
22. Zerbino, D. R., Wilder, S. P., Johnson, N., Juettemann, T. & Flicek, P. R. The Ensembl Regulatory Build. *Genome Biol.* **16**, 56 (2015).
23. Polo, J. M. *et al.* A Molecular Roadmap of Reprogramming Somatic Cells into iPS Cells. *Cell* **151**, 1617–1632 (2012).
24. David, L. & Polo, J. M. Phases of reprogramming. *Stem Cell Research* **12**, 754–761 (2014).
25. Meyer, D. H. & Schumacher, B. BiT age: A transcriptome-based aging clock near the theoretical limit of accuracy. *Aging Cell* **20**, e13320 (2021).
26. Humphrey, J. D., Dufresne, E. R. & Schwartz, M. A. Mechanotransduction and extracellular matrix homeostasis. *Nature Reviews Molecular Cell Biology* **15**, 802–812 (2014).
27. Varani, J. *et al.* Decreased collagen production in chronologically aged skin: Roles of age-dependent alteration in fibroblast function and defective mechanical stimulation. *Am. J. Pathol.* **168**, 1861–1868 (2006).
28. Lago, J. C. & Puzzi, M. B. The effect of aging in primary human dermal fibroblasts. *PLoS One* **14**, e0219165 (2019).
29. Li, B. & Wang, J. H.-C. Fibroblasts and myofibroblasts in wound healing: Force generation and measurement. *J. Tissue Viability* **20**, 108–120 (2011).
30. Ni, Z., Ebata, A., Alipanahiramandi, E. & Lee, S. S. Two SET domain containing genes link epigenetic changes and aging in Caenorhabditis elegans. *Aging Cell* **11**, 315–325 (2012).
31. O'Sullivan, R. J., Kubicek, S., Schreiber, S. L. & Karlseder, J. Reduced histone biosynthesis and chromatin changes arising from a damage signal at telomeres. *Nat. Struct. Mol. Biol.* **17**, 1218–1225 (2010).
32. Scaffidi, P. & Misteli, T. Lamin A-dependent nuclear defects in human aging. *Science (80-.).* **312**, 1059–1063 (2006).
33. Kerepesi, C., Zhang, B., Lee, S. G., Trapp, A. & Gladyshev, V. N. Epigenetic clocks reveal a rejuvenation event during embryogenesis followed by aging. *Sci. Adv.* **7**, (2021).
34. Weidner, C. *et al.* Aging of blood can be tracked by DNA methylation changes at just three CpG sites. *Genome Biol.* **15**, R24 (2014).
35. Lu, A. T. *et al.* DNA methylation-based estimator of telomere length. *Aging (Albany. NY).* **11**, 5895–5923 (2019).
36. Costantini, D. L. *et al.* The homeodomain transcription factor Irx5 establishes the mouse cardiac ventricular repolarization gradient. *Cell* **123**, 347–358 (2005).
37. Cheng, C. W. *et al.* The Iroquois homeobox gene, Irx5, is required for retinal cone bipolar cell development. *Dev. Biol.* **287**, 48–60 (2005).
38. Bu, D. F. *et al.* Two human glutamate decarboxylases, 65-kDa GAD and 67-kDa GAD, are each encoded by a single gene. *Proc. Natl. Acad. Sci.* **89**, 2115–2119 (1992).
39. Pearson, J. C., Lemons, D. & McGinnis, W. Modulating Hox gene functions during

animal body patterning. *Nat. Rev. Genet.* **6**, 893–904 (2005).
40. Zhang, H. *et al.* Structure and expression of fibrillin-2, a novel microfibrillar component preferentially located in elastic matrices. *J. Cell Biol.* **124**, 855–863 (1994).
41. Bristow, J., Tee, M., Gitelman, S., Mellon, S. & Miller, W. Tenascin-X: a novel extracellular matrix protein encoded by the human XB gene overlapping P450c21B. *J. Cell Biol.* **122**, 265–278 (1993).
42. Garbe, D. S., Das, A., Dubreuil, R. R. & Bashaw, G. J. β-Spectrin functions independently of Ankyrin to regulate the establishment and maintenance of axon connections in the Drosophila embryonic CNS. *Development* **134**, 273–284 (2007).
43. Grünberg, J. R., Hammarstedt, A., Hedjazifar, S. & Smith, U. The novel secreted adipokine wnt1-inducible signaling pathway protein 2 (WISP2) is a mesenchymal cell activator of canonical WNT. *J. Biol. Chem.* **289**, 6899–6907 (2014).
44. Janjanam, J. *et al.* Matricellular Protein WISP2 Is an Endogenous Inhibitor of Collagen Linearization and Cancer Metastasis. *Cancer Res.* **81**, 5666–5677 (2021).
45. Bitto, E., Bingman, C. A., Wesenberg, G. E., McCoy, J. G. & Phillips, G. N. Structure of aspartoacylase, the brain enzyme impaired in Canavan disease. *Proc. Natl. Acad. Sci.* **104**, 456–461 (2007).
46. Amengual, J. *et al.* STRA6 is critical for cellular vitamin A uptake and homeostasis. *Hum. Mol. Genet.* **23**, 5402–5417 (2014).
47. Hrvatin, S. *et al.* Differentiated human stem cells resemble fetal, not adult, β cells. *Proc. Natl. Acad. Sci.* **111**, 3038–3043 (2014).
48. Jadhav, U. *et al.* Extensive Recovery of Embryonic Enhancer and Gene Memory Stored in Hypomethylated Enhancer DNA. *Mol. Cell* **74**, 542-554.e5 (2019).
49. Schlaeger, T. M. *et al.* A comparison of non-integrating reprogramming methods. *Nat. Biotechnol.* **33**, 58–63 (2014).
50. Marion, R. M. *et al.* Telomeres Acquire Embryonic Stem Cell Characteristics in Induced Pluripotent Stem Cells. *Cell Stem Cell* **4**, 141–154 (2009).
51. Chondronasiou, D. *et al.* Multi-omic rejuvenation of naturally aged tissues by a single cycle of transient reprogramming. *Aging Cell* **21**, (2022).
52. Teshigawara, R., Cho, J., Kameda, M. & Tada, T. Mechanism of human somatic reprogramming to iPS cell. *Laboratory Investigation* **97**, 1152–1157 (2017).
53. Browder, K. C. *et al.* In vivo partial reprogramming alters age-associated molecular changes during physiological aging in mice. *Nat. Aging* **2**, 243–253 (2022).
54. Araki, Y. *et al.* Novel cadherin-related membrane proteins, Alcadeins, enhance the X11-like protein-mediated stabilization of amyloid beta-protein precursor metabolism. *J. Biol. Chem.* **278**, 49448–49458 (2003).
55. Ring, B. Z., Cordes, S. P., Overbeek, P. A. & Barsh, G. S. Regulation of mouse lens fiber cell development and differentiation by the Maf gene. *Development* **127**, 307–317 (2000).
56. Ohnishi, K. *et al.* Premature termination of reprogramming in vivo leads to cancer development through altered epigenetic regulation. *Cell* **156**, 663–677 (2014).
57. Cacchiarelli, D. *et al.* Integrative Analyses of Human Reprogramming Reveal Dynamic Nature of Induced Pluripotency. *Cell* **162**, 412–424 (2015).
58. Hockemeyer, D. *et al.* A drug-inducible system for direct reprogramming of human somatic cells to pluripotency. *Cell Stem Cell* **3**, 346–353 (2008).
59. Milagre, I. *et al.* Gender Differences in Global but Not Targeted Demethylation in iPSC Reprogramming. *Cell Rep.* **18**, 1079–1089 (2017).

60. Yang, Z. *et al.* Correlation of an epigenetic mitotic clock with cancer risk. *Genome Biol.* **17**, 205 (2016).
61. Lu, A. T. *et al.* DNA methylation GrimAge strongly predicts lifespan and healthspan. *Aging (Albany. NY).* **11**, 303–327 (2019).
62. Levine, M. E. *et al.* An epigenetic biomarker of aging for lifespan and healthspan. *Aging (Albany. NY).* **10**, 573–591 (2018).
63. McEwen, L. M. *et al.* Systematic evaluation of DNA methylation age estimation with common preprocessing methods and the Infinium MethylationEPIC BeadChip array. *Clin. Epigenetics* **10**, 123 (2018).
64. Santos, F. *et al.* Epigenetic Marking Correlates with Developmental Potential in Cloned Bovine Preimplantation Embryos. *Curr. Biol.* **13**, 1116–1121 (2003).
65. Kuhn, M. Building predictive models in R using the caret package. *J. Stat. Softw.* **28**, 1–26 (2008).

Figure legends

Figure 1. Transiently reprogrammed cells reacquire their initial cellular identity

(A) Mean DNA methylation age (calculated using the multi-tissue clock [3]) throughout the reprogramming process where cells were transduced with our tetO-GFP-hOKMS vector and treated continuously with 2 µg/mL of doxycycline. Reprogramming is divided in three distinct phases: initiation phase (IP); maturation phase (MP) and stabilisation phase (SP). DNA methylation age decreased substantially during the maturation phase of reprogramming in cells that were successfully reprogramming (magenta line) but not in control cells (yellow and orange lines represent non-transduced cells and cells expressing hOKMS but failing to reprogram as indicated by cell surface markers, respectively). Points represent the mean and error bars the standard deviation. N = 3 biological replicates per condition, where fibroblasts were derived from different donors. N = 2 biological replicates for the iPSC timepoint (day 51).

(B) Experimental scheme for maturation phase transient reprogramming (MPTR). The tetO-GFP-hOKMS reprogramming construct was introduced into fibroblasts from older donors by lentiviral transduction. Alternatively, cells were 'mock infected' as a negative control. Following this, cells were grown in the presence of 2 µg/mL doxycycline to initiate reprogramming. At several timepoints during the maturation phase, cells were flow sorted and successfully reprogramming cells (CD13- SSEA4+) and cells that were failing to reprogram (CD13+ SSEA4-) were collected for analysis. These were termed "transient reprogramming intermediate" and "failing to transiently reprogram intermediate", respectively. Sorted cells were also further cultured, and grown in the absence of doxycycline for at least four weeks - these were termed "transiently reprogrammed" (CD13- SSEA4+) or "failed to transiently reprogram" (CD13+ SSEA4-).

(C) Phase-contrast microscope images of cells after doxycycline treatment (transient reprogramming intermediate) and after withdrawal of doxycycline (transiently reprogrammed) as described in B. The morphology of some cells changed after doxycycline treatment. These cells appeared to form colonies, which became larger with longer exposure to doxycycline. After sorting, these cells were cultured in medium no longer containing doxycycline, and appeared to return to their initial fibroblast morphology.

(D) Roundness ratio of cells before, during and after MPTR (with 13 days of reprogramming). Roundness ratio was calculated by dividing maximum length by perpendicular width. Fibroblasts became significantly rounder during MPTR and returned to a more elongated upon the completion of MPTR. Values from individual cells have been represented as violin plots. Points represent mean values and are connected with lines. Significance was calculated with a Tukey's range test. Representative 3D renderings of cells (generated using Volocity) before, during and after successful transient reprogramming are included below the plot. CD13 is coloured in green, SSEA4 is coloured in red and DAPI staining is coloured in blue. White scale bars represent a distance of 20 µm.

(E) Principal component analysis of transient reprogramming and reference reprogramming sample transcriptomes (light blue to dark blue and black crosses, data from Banovich et al[20], Fleischer et al[5] and our novel Sendai reprogramming dataset). Reference samples form a reprogramming trajectory along PC1. In the Sendai reprogramming reference dataset, cells that were not reprogramming (CD13+ SSEA4-) were also profiled and clustered midway along PC1 suggesting some transcriptional changes had still occurred in these cells. Transient reprogramming samples moved along this trajectory with continued exposure to doxycycline (light magenta points) and returned to the beginning of the trajectory after withdrawal of doxycycline (magenta points). Control samples (yellow and orange points) remained at the beginning of the trajectory throughout the experiment.

(F) Mean gene expression levels for the fibroblast specific gene *FSP1* and the iPSC specific gene *NANOG*. Transiently reprogrammed samples expressed these genes at levels similar to control fibroblasts. Bars represent the mean and error bars the standard deviation. Samples transiently reprogrammed for 13, 15 or 17 days were pooled. The number of distinct samples in each group is indicated in brackets.

(G) Principal component analysis of transient reprogramming (magenta points) and reference reprogramming sample methylomes (light blue to dark blue and black crosses, data from Banovich et al[20], Ohnuki et al[19] and our novel Sendai reprogramming dataset). Reference samples formed a reprogramming trajectory along PC1. Transient reprogramming samples moved along this trajectory with continued exposure to doxycycline (light magenta points) and returned to the beginning of the trajectory after withdrawal of doxycycline (magenta points). Control samples (yellow and orange points) remained at the beginning of the trajectory throughout the experiment.

(H) Mean DNA methylation levels across the fibroblast specific gene *FSP1* and the iPSC specific gene *POU5F1* (encoding OCT4). Transiently reprogrammed samples had methylation profiles across these genes that resemble those found in fibroblasts. Grey bars and black bars indicate the locations of Ensembl annotated

promoters and genes, respectively. Samples transiently reprogrammed for 10, 13, 15 or 17 days were pooled for visualisation purposes. The number of distinct samples in each group is indicated in brackets.

Figure 2. Epigenetic memory at enhancers and persistent fibroblast gene expression may allow cells to return to their initial identity

(A) The mean expression levels of fibroblast-specific and iPSC-specific gene sets during transient reprogramming and complete reprogramming. Error bars represent the standard deviation.

(B) Heatmap examining the expression of fibroblast-specific genes in cells before (light blue group), during (light magenta group, transient reprogramming intermediate cells) and after (magenta group, transiently reprogrammed fibroblasts) transient reprogramming as well as in iPSCs (dark blue group). The number of days of reprogramming is indicated above the heatmap where applicable. The majority of fibroblast genes are downregulated at the intermediate stages of transient reprogramming. However, some fibroblast genes are persistently expressed or temporarily upregulated at this stage.

(C) Mean DNA methylation levels across enhancers linked to the three clusters of fibroblast genes during transient reprogramming and complete reprogramming. DNA methylation levels across enhancers remain unchanged during transient reprogramming regardless of the expression of their associated genes. In comparison, DNA methylation levels across these regions increase during complete reprogramming. Error bars represent the standard deviation.

(D) Heatmap examining the DNA methylation levels of fibroblast-specific enhancers in cells before (light blue group), during (light magenta group) and after (magenta group) transient reprogramming as well as in iPSCs (dark blue group). Each sample was plotted as a single column, whether reprogrammed for 10, 13, 15, or 17 days. Fibroblast enhancers became hypermethylated during complete reprogramming but were still demethylated at the intermediate stages of transient reprogramming. Fibroblast-specific enhancers were defined as enhancers that are active in fibroblasts but no longer active in iPSCs (become inactive, poised or repressed) based on Ensembl regulatory build annotations.

(E) The mean expression and enhancer methylation levels of example genes during transient reprogramming and complete reprogramming. MMP1 is a gene that demonstrates epigenetic memory as it is temporarily downregulated during transient reprogramming and its enhancer remains demethylated. COL1A2 is a gene that demonstrates transcriptional persistence as it remains expressed throughout transient reprogramming.

Figure 3. Transient reprogramming reverses age-associated changes in the transcriptome and partially restores fibroblast migration speed.

(A) Principal component analysis of fibroblast ageing-associated gene expression levels in transient reprogramming (magenta) and reference ageing fibroblast samples (light blue-dark blue). Reference samples formed an ageing trajectory along PC1. Transiently reprogrammed samples located closer to young fibroblasts than negative control samples did (yellow and orange), suggesting they were transcriptionally younger.

(B) PC1 values from the principal component analysis of fibroblast ageing-associated gene expression levels and their equivalent age based on the reference ageing fibroblast samples. PC1 values were greater in transiently reprogrammed samples than negative control and failed to transiently reprogram samples and as result these samples appear to be younger. Bars represent the mean and error bars represent the standard deviation.

(C) Mean transcription age calculated using a custom transcriptome clock (median absolute error=12.57 years) for negative control samples (yellow), samples that expressed OSKM but failed to reprogram based on cell surface markers (orange) and cells that were successfully transiently reprogrammed (magenta) as described in Figure 1B for 10, 13, 15 or 17 days. The number of distinct samples in each group is indicated in brackets. Bars represent the mean and error bars the standard deviation. Statistical significance was calculated with Mann-Whitney U tests.

(D) The mean expression levels of all genes in transiently reprogrammed samples with 13 days of reprogramming compared to those in corresponding negative control samples. In addition, genes have been colour coded by their expression change with age. Genes that upregulate with age were downregulated with transient reprogramming and genes that downregulate with age were upregulated with transient reprogramming. Notable example genes have been highlighted. The number of distinct samples in each group is indicated in brackets.

(E) The expression levels of collagen genes that were restored to youthful levels after transient reprogramming with 13 days of reprogramming. Bars represent the mean and error bars the standard deviation. The number of distinct samples in each group is indicated in square brackets. Significance was calculated with a two-sided Mann-Whitney U test.

(F) Boxplots of the protein levels of Collagen I and IV in individual cells after transient reprogramming for 10 or 13 days calculated based on fluorescence intensity within segmented cells following immunofluorescence staining. Boxes represent upper and lower quartiles and central lines the median. The protein levels of Collagen I and IV increased after transient reprogramming. The number of distinct samples in each group is indicated in square brackets. Representative images are included (bottom panel). CD44 is coloured in green, Collagen I and IV are coloured in red and DAPI staining is coloured in blue. Significance was calculated with a two-sided Mann-Whitney U test.
(G) The migration speed of fibroblasts in a wound healing assay. Migration speed was significantly lower in negative control fibroblasts from middle-aged donors compared to fibroblasts from young donors (aged 20-22). Transient reprogramming improved the migration speed in some samples but had no effect in others. Technical replicates were averaged, and the mean values have been presented as boxplots where the boxes represent the upper and lower quartiles and the central lines the median. Significance was calculated with a Tukey's range test.

Figure 4. Optimal transient reprogramming can reverse age-associated changes in the epigenome
A) Boxplots of the levels of H3K9me3 in individual cells calculated based on fluorescence intensity within nuclei (segmented using DAPI). The levels of H3K9me3 were found to decrease with age and increase after transient reprogramming for 10 or 13 days. Boxes represent upper and lower quartiles and central lines the median. The number of distinct samples in each group is indicated in square brackets. Representative images are included (right panel). H3K9me3 is coloured in green and DAPI staining is coloured in greyscale. Significance was calculated with a two-sided Mann-Whitney U test.
(B) Mean DNA methylation age of samples after transient reprogramming calculated using the multi-tissue clock[3]. DNA methylation age substantially reduced after 13 days of transient reprogramming. Shorter and longer lengths of transient reprogramming led to smaller reductions in DNA methylation age. Bars represent the mean and error bars represent the standard deviation. The outlier in the 13 days of transient reprogramming group was excluded from calculation of the mean and standard deviation. Significance was calculated with a two-sided Mann-Whitney U test with (in brackets) and without the outlier. The number of distinct samples in each group is indicated in brackets beneath the bars.
(C) Mean telomere length of samples after transient reprogramming calculated using the telomere length clock 31. Telomere length either did not change or was slightly reduced after transient reprogramming. Bars represent the mean and error bars represent the standard deviation. Significance was calculated with a two-sided Mann-Whitney U test.
(D) Mean DNA methylation levels across a rejuvenated age-hypomethylated region. This region is found within the IRX5 promoter. Samples transiently reprogrammed for 13 days were pooled for visualisation purposes. The number of distinct samples in each group is indicated in brackets.
(E) Mean DNA methylation levels across rejuvenated age-hypermethylated regions. These regions are found within the GAD1 promoter and HOXB locus. Samples transiently reprogrammed for 13 days were pooled for visualisation purposes. The number of distinct samples in each group is indicated in brackets.
(F) The overlap in rejuvenated methylation CpG sites and rejuvenated expression genes. Rejuvenated CpG sites were annotated with the nearest gene for this overlap analysis. The universal set was restricted to genes that were annotated to CpG sites in the DNA methylation array. Fisher's exact test was used to calculate the significance of the overlap. The six genes that were found in both sets are listed along with the direction of their DNA methylation (red) and gene expression (blue) change with age.

Figure supplement legends

Figure 1-figure supplement 1

(A) Mean DNA methylation age (calculated using multiple epigenetic clocks[2,18,34,60–62]) throughout the reprogramming process where cells were transduced with our tetO-GFP-hOKMS vector and treated continuously with 2 µg/mL of doxycycline. Reprogramming is divided into three distinct phases: initiation phase (IP); maturation phase (MP) and stabilisation phase (SP). DNA methylation age according to the skin and blood clock decreased substantially during the maturation phase of reprogramming in cells that were successfully reprogramming (magenta line) but not in control cells (yellow and orange lines represent non-transduced cells and cells expressing hOKMS but failing to reprogram as indicated by cell surface markers, respectively). DNA methylation age decreased substantially during the stabilisation phase for other epigenetic clocks and was unaffected by reprogramming for the epiTOC clock. Points represent the mean and error bars the standard deviation. N = 3 biological replicates per condition, where fibroblasts were derived from different donors. N = 2 biological replicates for the iPSC timepoint (day 51).

(B) The percentage of cells measured in each quadrant during the flow sort for successfully reprogramming cells (top panel). Cells were classified as CD13 only (CD13+ SSEA4-), double negative ("DN", CD13- SSEA4-), double positive ("DP", CD13+ SSEA4+) or SSEA4 only (CD13- SSEA4+). Cells that were collected are colour coded (light yellow = negative control intermediate, light orange = failed to transiently reprogram intermediate, light magenta = transient reprogramming intermediate). Bars represent the mean and error bars the standard deviation. Representative flow cytometry plots (bottom panel) show where gates were placed for determining presence/absence of surface markers.

(C) Representative 3D renderings of cells (generated using Volocity) that failed to transiently reprogram or were negative controls at the start, intermediate and end stages of MPTR. CD13 is coloured in green, SSEA4 is coloured in red and DAPI staining is coloured in blue. White scale bars represent a distance of 20 µm.

(D) Principal component analysis of the transcriptomes of the samples generated in this study (without reference datasets). PC1 separates the starting fibroblasts from fully reprogrammed iPSCs. Transient reprogramming intermediate samples cluster closer to iPSCs than fibroblasts. Upon completion of transient reprogramming, samples cluster again with fibroblasts.

(E) Principal component analysis of the DNA methylomes of the samples generated in this study (without reference datasets). PC1 separates the starting fibroblasts from fully reprogrammed iPSCs. Transient reprogramming intermediate samples cluster in between iPSCs and fibroblasts. Upon completion of transient reprogramming, samples cluster again with fibroblasts.

Figure 2-figure supplement 1

(A) Volcano plot showing the differentially expressed genes between iPSCs and fibroblasts. Differentially expressed genes were determined with DESeq2 ($P \leq 0.05$ and log2 fold change ≤ 1). In this comparison, upregulated genes were classed as iPSC-specific genes and downregulated genes were classed as fibroblast-specific genes.

(B) Heatmap examining the expression of fibroblast-specific genes in cells before (light blue group), during (light magenta group, transient reprogramming intermediate cells) and after (magenta group, transiently reprogrammed fibroblasts) transient reprogramming. Fibroblast genes were divided into three clusters, which displayed different expression patterns during transient reprogramming. The number of genes within each cluster is shown in brackets.

(C) Heatmap examining the expression of iPSC-specific genes in cells before (light blue group), during (light magenta group, transient reprogramming intermediate cells) and after (magenta group, transiently reprogrammed fibroblasts) transient reprogramming as well as in iPSCs (dark blue group). The number of days of reprogramming is indicated above the heatmap where applicable.

(D) Mean DNA methylation levels across promoters linked to the three clusters of fibroblast genes during transient reprogramming and complete reprogramming. DNA methylation levels across promoters remained lowly methylated during transient reprogramming and complete reprogramming regardless of the expression of their associated genes. Error bars represent the standard deviation.

(E) Heatmaps examining the DNA methylation levels of enhancers linked to the three clusters of fibroblast genes in cells before (light blue group), during (light magenta group) and after (magenta group) transient reprogramming as well as in iPSCs (dark blue group). For all three clusters, a subset of enhancers was still demethylated at the intermediate stages of transient reprogramming but became hypermethylated during complete reprogramming.

Figure 3-figure supplement 1

(A) Results of the tenfold cross validation comparing predicted age to actual age for a custom transcriptome clock.

(B) Mean transcription age calculated using a custom transcriptome clock (median absolute error=12.57 years) for initiation phase transiently reprogrammed fibroblasts[15]. The number of distinct samples in each group is indicated in brackets. Bars represent the mean and error bars the standard deviation.

(C) Mean transcription age calculated using the retrained BiT age clock (median absolute error=5.55 years) for negative control samples (yellow), samples that expressed OSKM but failed to reprogram based on cell surface markers (orange) and cells that were successfully transiently reprogrammed (magenta) for 10, 13, 15 or 17 days. The number of distinct samples in each group is indicated in brackets. Bars represent the mean and error bars the standard deviation. Statistical significance was calculated with Mann-Whitney U tests.

(D) The expression levels of notable genes that were restored to youthful levels after transient reprogramming with 13 days of reprogramming. Bars represent the mean and error bars the standard deviation. The number of distinct samples in each group is indicated in square brackets.

(E) Migration speed of the technical replicates in a wound healing assay. Matched samples from the same starting population of fibroblasts (biological replicates) have been grouped (separated by dashed lines). In addition, the migration speeds of fibroblasts from four young control donors have been provided for comparison. In two cases, transient reprogramming improved the migration speed of fibroblasts and in two cases transient reprogramming appeared to have no effect on migration speed.

Figure 4-figure supplement 1

(A) The expression levels of DNA methyltransferases and TET enzymes throughout the reprogramming process where cells were transduced with our tetO-GFP-hOKMS vector and treated continuously with 2 µg/mL of doxycycline. Reprogramming is divided into three distinct phases: initiation phase (IP); maturation phase (MP) and stabilisation phase (SP). The *de novo* methyltransferases and TET enzymes are upregulated during the maturation phase relative to negative controls. N = 3 biological replicates per condition, where fibroblasts were derived from different donors. N = 2 biological replicates for the day 17 reprogramming timepoint and the iPSC timepoint (day 51).

(B) Mean DNA methylation age of samples after transient reprogramming calculated using multiple epigenetic clocks[2,18,34,60–62]. DNA methylation age substantially reduced after 13 days of transient reprogramming for the skin and blood clock and the Weidner clock. Shorter and longer lengths of transient reprogramming led to smaller reductions in DNA methylation age. Other epigenetic clocks were unaffected by the four lengths of transient reprogramming. Bars represent the mean and error bars represent the standard deviation. Significance was calculated with the Mann-Whitney U test. The number of distinct samples in each group is indicated in brackets.

(C) Mean telomere length (calculated using the telomere length clock[35]) throughout the reprogramming process where cells were transduced with our tetO-GFP-hOKMS vector and treated continuously with 2 µg/mL of doxycycline. Reprogramming is divided into three distinct phases: initiation phase (IP); maturation phase (MP) and stabilisation phase (SP). Telomere length decreases during the initiation and maturation phases and begins to increase during the stabilisation phase. Points represent the mean and error bars the standard deviation. N = 3 biological replicates per condition, where fibroblasts were derived from different donors. N = 2 biological replicates for the iPSC timepoint (day 51).

(D) The expression of TERT throughout the reprogramming process where cells were transduced with our tetO-GFP-hOKMS vector. Reprogramming is divided into three distinct phases: initiation phase (IP); maturation phase (MP) and stabilisation phase (SP). Points represent the mean and error bars the standard deviation. TERT expression begins to increase during the maturation phase and is weakly expressed at the end of the maturation phase. TERT expression continues to increase during the stabilisation phase. N = 3 biological replicates per condition, where fibroblasts were derived from different donors. N = 2 biological replicates for the day 17 reprogramming timepoint and the iPSC timepoint (day 51).

(E) The location of rejuvenated CpG sites after 13 days of transient reprogramming. Sites rejuvenated by demethylation are coloured in blue and sites rejuvenated by methylation are coloured in pink.

Supplementary file legends

Supplementary file 1

A comparison of previous transient reprogramming methods.

Supplementary file 2

The complete results of the Tukey's range test that was used to compare the morphology ratio between the different stages and groups of MPTR.

Supplementary file 3

The lists of fibroblast genes that were identified to either temporarily downregulate, temporarily upregulate or persist in their expression during MPTR.

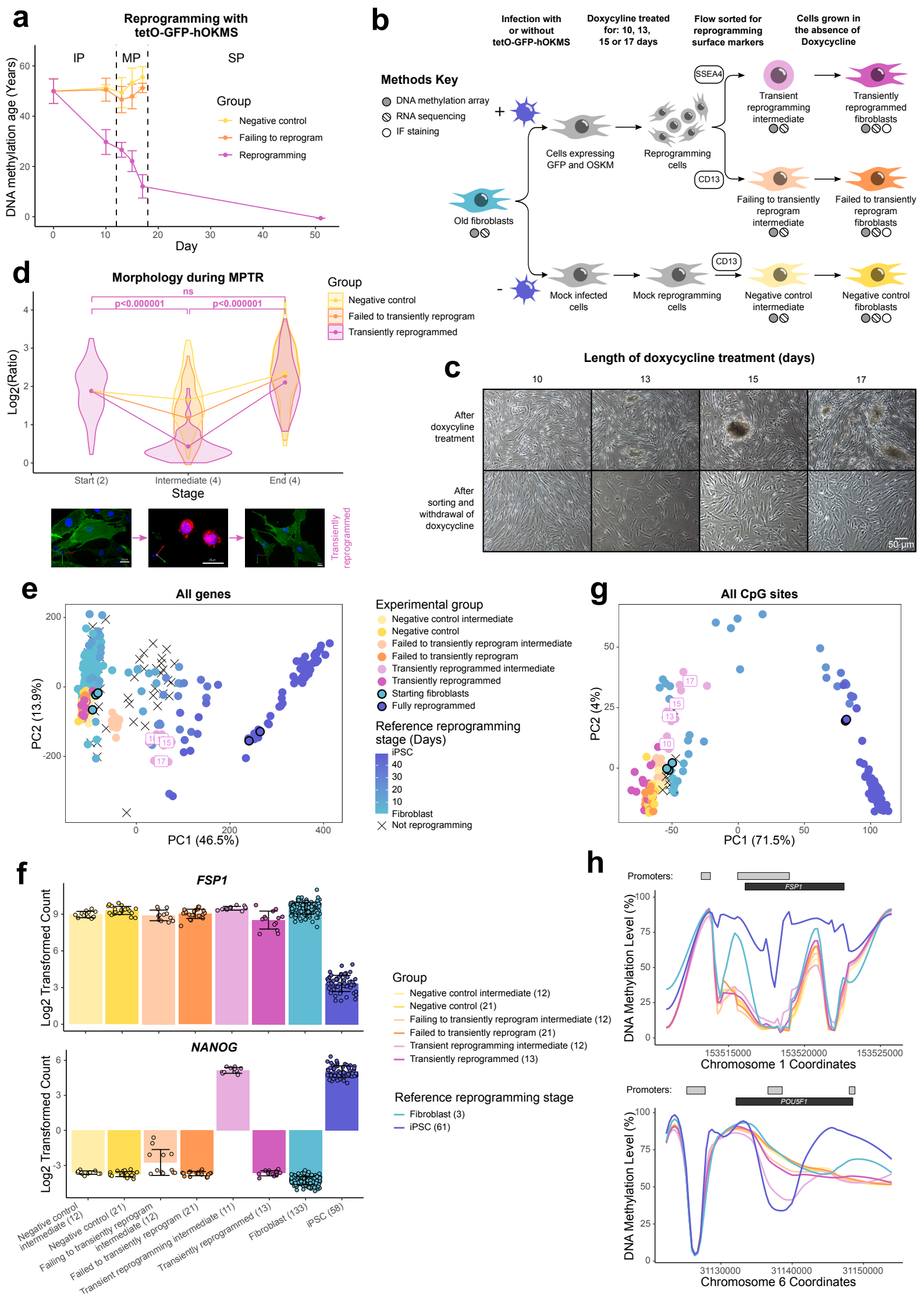
a
Reprogramming with tetO-GFP-hOKMS
IP
MP
SP
Group
Negative control
Failing to reprogram
Reprogramming
DNA methylation age (Years)
Day
b
Infection with or without tetO-GFP-hOKMS
Doxycyline treated for: 10, 13, 15 or 17 days
Flow sorted for reprogramming surface markers
Cells grown in the absence of Doxycycline
Methods Key
DNA methylation array
RNA sequencing
IF staining
Old fibroblasts
Cells expressing GFP and OSKM
Reprogramming cells
SSEA4
Transient reprogramming intermediate
Transiently reprogrammed fibroblasts
CD13
Failing to transiently reprogram intermediate
Failed to transiently reprogram fibroblasts
Mock infected cells
Mock reprogramming cells
Negative control intermediate
Negative control fibroblasts
c
Length of doxycycline treatment (days)
10
13
15
17
After doxycyline treatment
After sorting and withdrawal of doxycycline
50 µm
d
Morphology during MPTR
ns
p<0.000001
p<0.000001
Log2(Ratio)
Start (2)
Intermediate (4)
End (4)
Stage
Group
Negative control
Failed to transiently reprogram
Transiently reprogrammed
Transiently reprogrammed
e
All genes
PC2 (13.9%)
PC1 (46.5%)
Experimental group
Negative control intermediate
Negative control
Failed to transiently reprogram intermediate
Failed to transiently reprogram
Transiently reprogrammed intermediate
Transiently reprogrammed
Starting fibroblasts
Fully reprogrammed
Reference reprogramming stage (Days)
iPSC
40
30
20
10
Fibroblast
Not reprogramming
g
All CpG sites
PC2 (4%)
PC1 (71.5%)
f
FSP1
NANOG
Log2 Transformed Count
Negative control intermediate (12)
Negative control (21)
Failing to transiently reprogram intermediate (12)
Failed to transiently reprogram (21)
Transient reprogramming intermediate (11)
Transiently reprogrammed (13)
Fibroblast (133)
iPSC (58)
Group
Negative control intermediate (12)
Negative control (21)
Failing to transiently reprogram intermediate (12)
Failed to transiently reprogram (21)
Transient reprogramming intermediate (12)
Transiently reprogrammed (13)
Reference reprogramming stage
Fibroblast (3)
iPSC (61)
h
Promoters:
FSP1
DNA Methylation Level (%)
Chromosome 1 Coordinates
153515000
153520000
153525000
Promoters:
POU5F1
DNA Methylation Level (%)
Chromosome 6 Coordinates
31130000
31140000
31150000

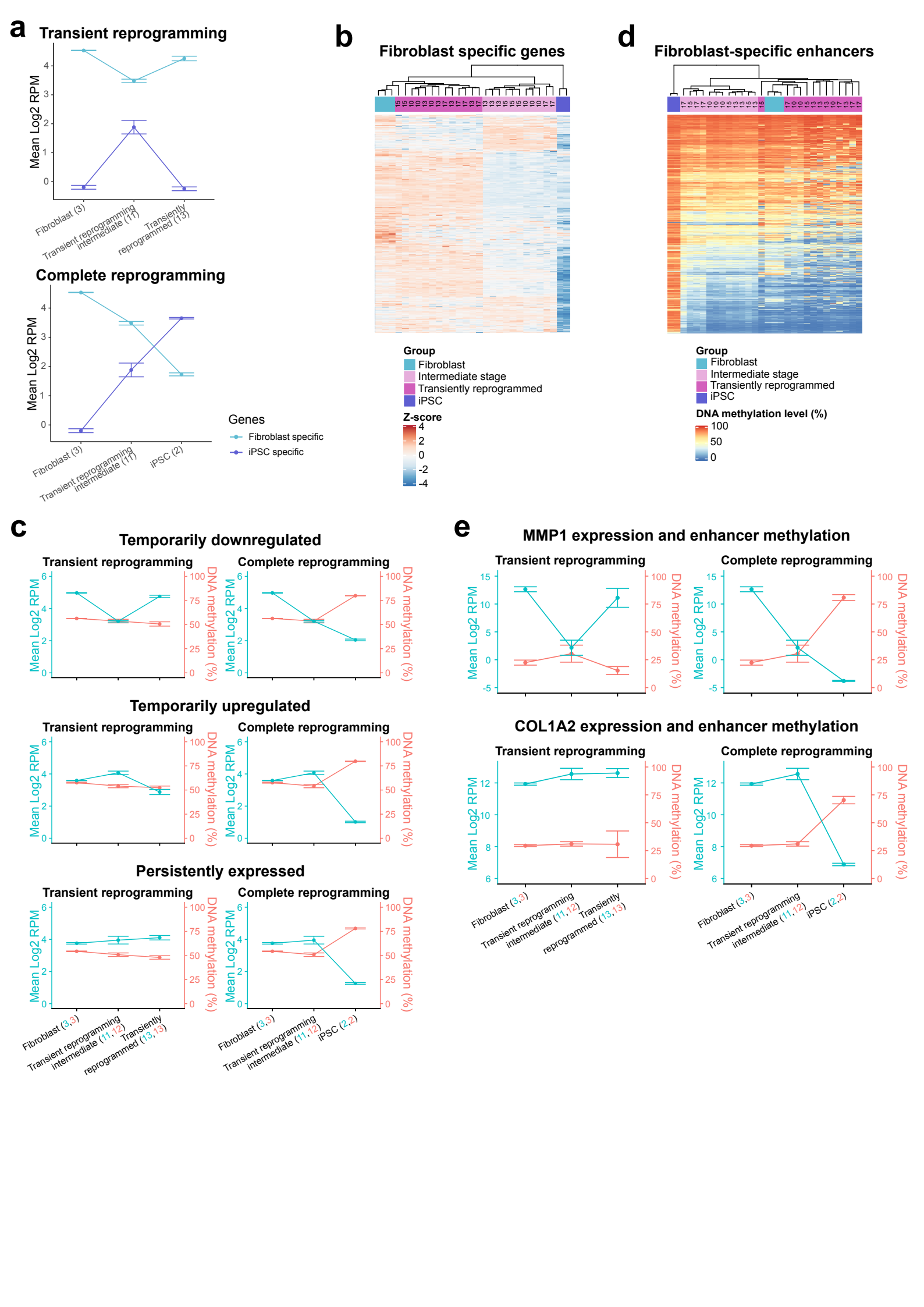
a
Transient reprogramming
Mean Log2 RPM
Fibroblast (3)
Transient reprogramming intermediate (11)
Transiently reprogrammed (13)
Complete reprogramming
iPSC (2)
Genes
Fibroblast specific
iPSC specific
b
Fibroblast specific genes
Group
Fibroblast
Intermediate stage
Transiently reprogrammed
iPSC
Z-score
d
Fibroblast-specific enhancers
DNA methylation level (%)
c
Temporarily downregulated
Temporarily upregulated
Persistently expressed
DNA methylation (%)
e
MMP1 expression and enhancer methylation
COL1A2 expression and enhancer methylation

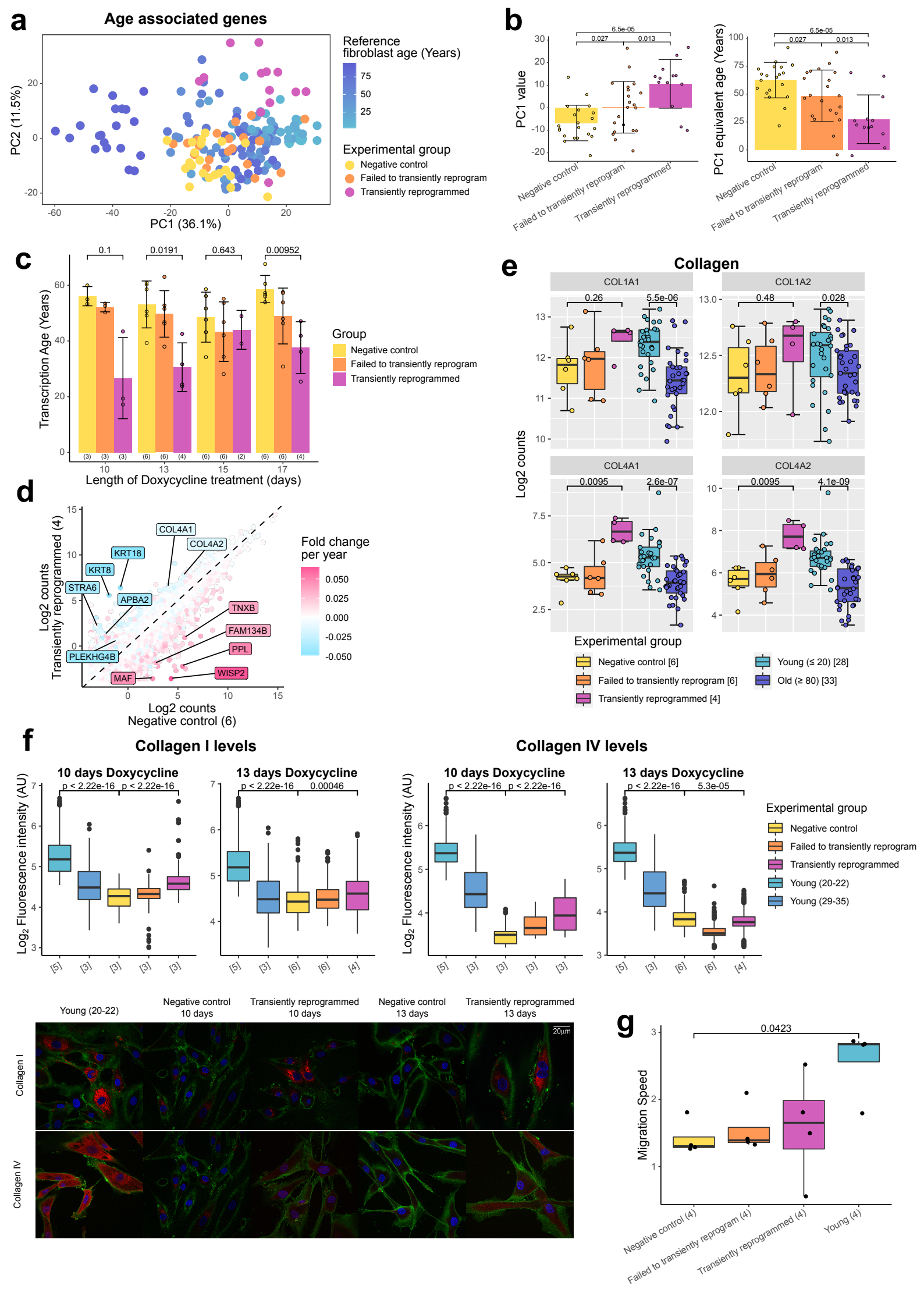
a
Age associated genes
PC2 (11.5%)
PC1 (36.1%)
Reference fibroblast age (Years)
75
50
25
Experimental group
Negative control
Failed to transiently reprogram
Transiently reprogrammed
b
PC1 value
PC1 equivalent age (Years)
6.5e-05
0.027
0.013
Negative control
Failed to transiently reprogram
Transiently reprogrammed
c
Transcription Age (Years)
0.1
0.0191
0.643
0.00952
Length of Doxycycline treatment (days)
Group
Negative control
Failed to transiently reprogram
Transiently reprogrammed
d
Log2 counts Transiently reprogrammed (4)
Log2 counts Negative control (6)
COL4A1
COL4A2
KRT18
KRT8
STRA6
APBA2
TNXB
FAM134B
PPL
PLEKHG4B
MAF
WISP2
Fold change per year
0.050
0.025
0.000
-0.025
-0.050
e
Collagen
COL1A1
COL1A2
COL4A1
COL4A2
Log2 counts
0.26
5.5e-06
0.48
0.028
0.0095
2.6e-07
0.0095
4.1e-09
Experimental group
Negative control [6]
Failed to transiently reprogram [6]
Transiently reprogrammed [4]
Young (≤ 20) [28]
Old (≥ 80) [33]
f
Collagen I levels
Collagen IV levels
10 days Doxycycline
13 days Doxycycline
Log2 Fluorescence intensity (AU)
p < 2.22e-16
0.00046
5.3e-05
Experimental group
Negative control
Failed to transiently reprogram
Transiently reprogrammed
Young (20-22)
Young (29-35)
Young (20-22)
Negative control 10 days
Transiently reprogrammed 10 days
Negative control 13 days
Transiently reprogrammed 13 days
Collagen I
Collagen IV
20μm
g
Migration Speed
0.0423
Negative control (4)
Failed to transiently reprogram (4)
Transiently reprogrammed (4)
Young (4)

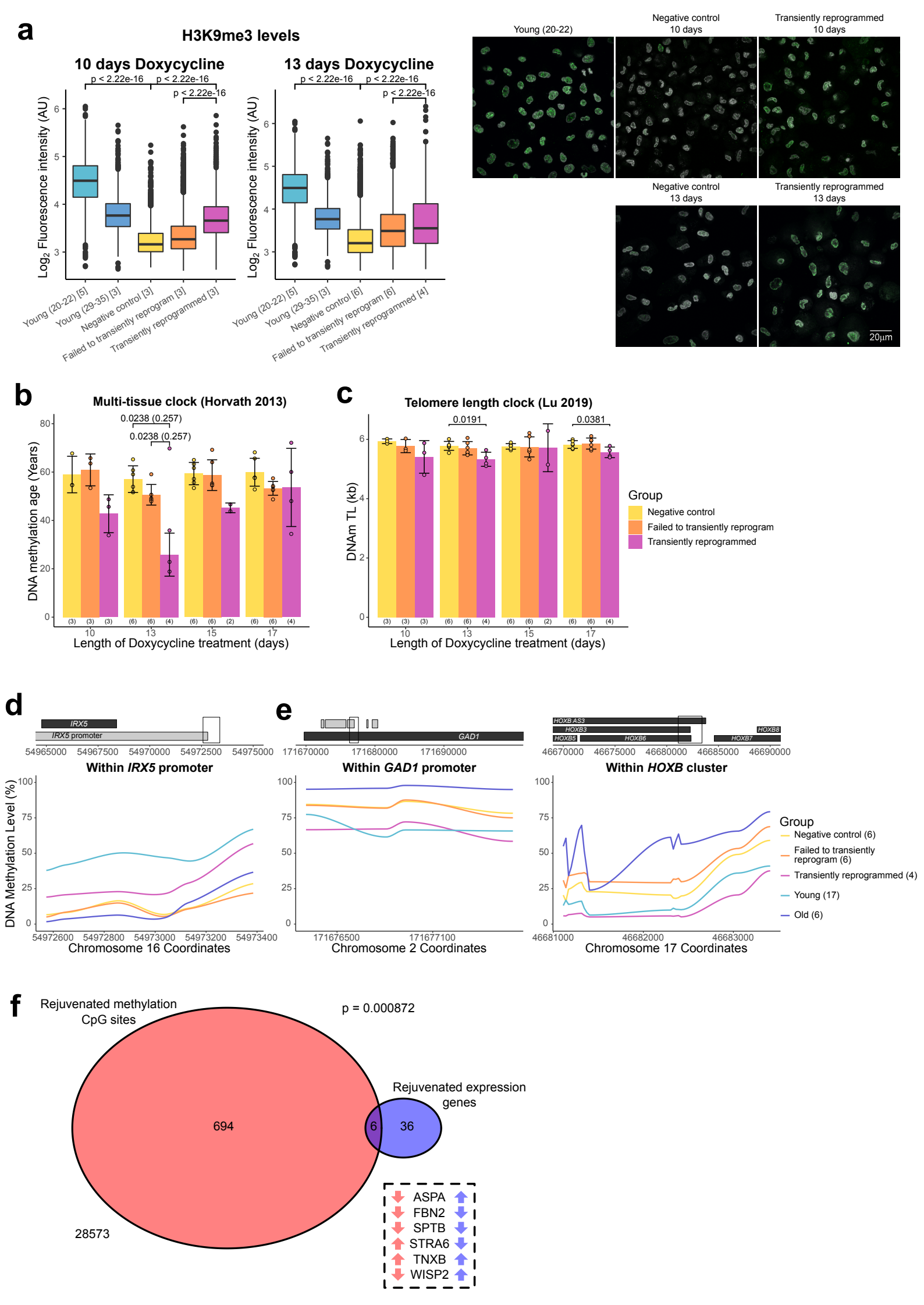
a
H3K9me3 levels
10 days Doxycycline
13 days Doxycycline
p < 2.22e-16
Log2 Fluorescence intensity (AU)
Young (20-22) [5]
Young (29-35) [3]
Negative control [3]
Failed to transiently reprogram [3]
Transiently reprogrammed [3]
Negative control [6]
Failed to transiently reprogram [6]
Transiently reprogrammed [4]
Young (20-22)
Negative control 10 days
Transiently reprogrammed 10 days
Negative control 13 days
Transiently reprogrammed 13 days
20μm
b
Multi-tissue clock (Horvath 2013)
0.0238 (0.257)
DNA methylation age (Years)
Length of Doxycycline treatment (days)
c
Telomere length clock (Lu 2019)
0.0191
0.0381
DNAm TL (kb)
Group
Negative control
Failed to transiently reprogram
Transiently reprogrammed
d
IRX5
IRX5 promoter
Within IRX5 promoter
DNA Methylation Level (%)
Chromosome 16 Coordinates
e
GAD1
Within GAD1 promoter
Chromosome 2 Coordinates
HOXB AS3
HOXB3
HOXB5
HOXB6
HOXB8
HOXB7
Within HOXB cluster
Chromosome 17 Coordinates
Group
Negative control (6)
Failed to transiently reprogram (6)
Transiently reprogrammed (4)
Young (17)
Old (6)
f
Rejuvenated methylation CpG sites
p = 0.000872
Rejuvenated expression genes
694
6
36
28573
ASPA
FBN2
SPTB
STRA6
TNXB
WISP2

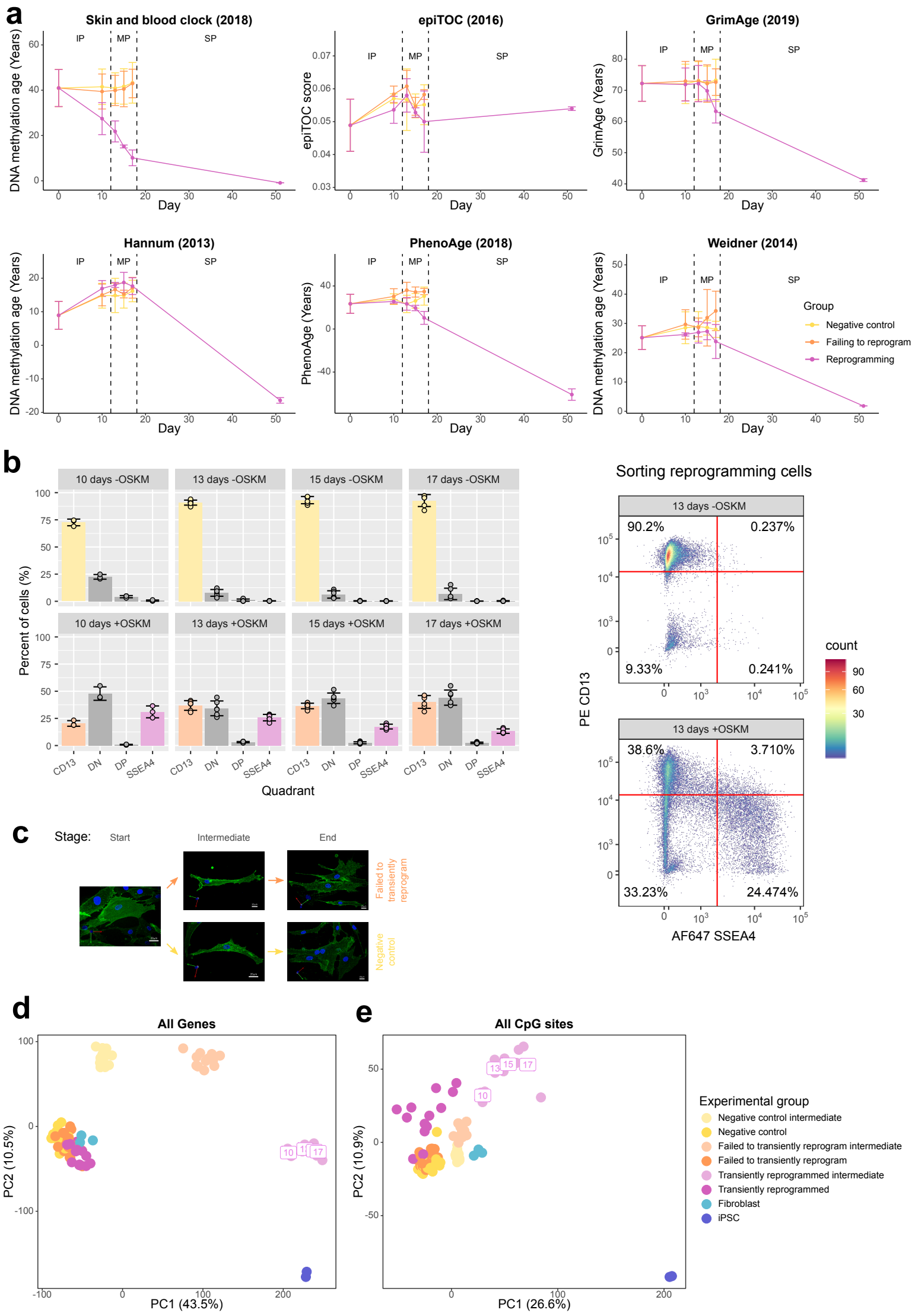
a
Skin and blood clock (2018)
epiTOC (2016)
GrimAge (2019)
Hannum (2013)
PhenoAge (2018)
Weidner (2014)
IP
MP
SP
DNA methylation age (Years)
epiTOC score
GrimAge (Years)
PhenoAge (Years)
Day
Group
Negative control
Failing to reprogram
Reprogramming
b
10 days -OSKM
13 days -OSKM
15 days -OSKM
17 days -OSKM
10 days +OSKM
13 days +OSKM
15 days +OSKM
17 days +OSKM
Percent of cells (%)
CD13
DN
DP
SSEA4
Quadrant
Sorting reprogramming cells
90.2%
0.237%
9.33%
0.241%
38.6%
3.710%
33.23%
24.474%
PE CD13
AF647 SSEA4
count
c
Stage:
Start
Intermediate
End
Failed to transiently reprogram
Negative control
d
All Genes
PC1 (43.5%)
PC2 (10.5%)
e
All CpG sites
PC1 (26.6%)
PC2 (10.9%)
Experimental group
Negative control intermediate
Negative control
Failed to transiently reprogram intermediate
Failed to transiently reprogram
Transiently reprogrammed intermediate
Transiently reprogrammed
Fibroblast
iPSC

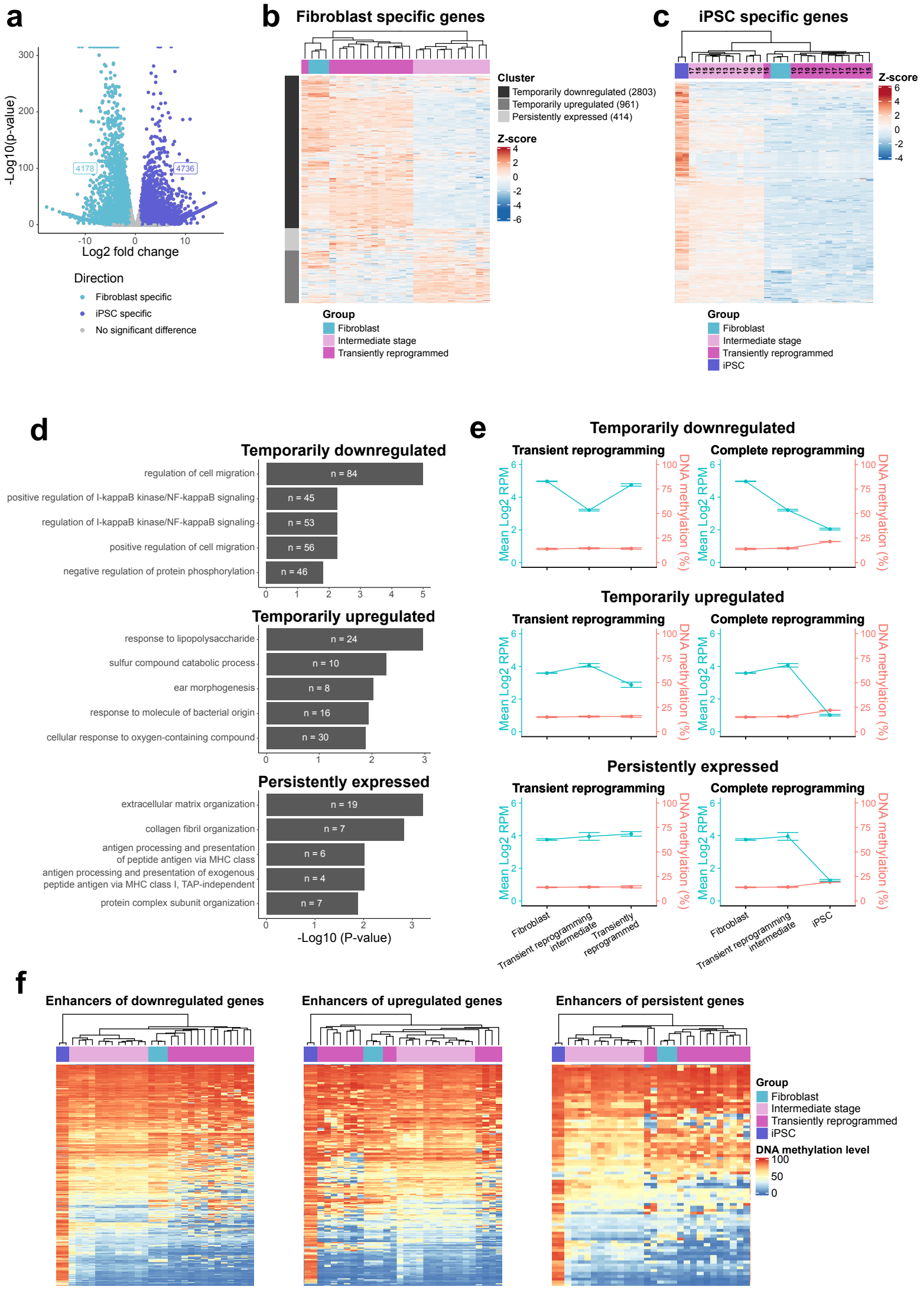
a
-Log10(p-value)
Log2 fold change
4178
4736
Direction
Fibroblast specific
iPSC specific
No significant difference
b
Fibroblast specific genes
Cluster
Temporarily downregulated (2803)
Temporarily upregulated (961)
Persistently expressed (414)
Z-score
Group
Fibroblast
Intermediate stage
Transiently reprogrammed
c
iPSC specific genes
Z-score
Group
Fibroblast
Intermediate stage
Transiently reprogrammed
iPSC
d
Temporarily downregulated
regulation of cell migration
positive regulation of I-kappaB kinase/NF-kappaB signaling
regulation of I-kappaB kinase/NF-kappaB signaling
positive regulation of cell migration
negative regulation of protein phosphorylation
Temporarily upregulated
response to lipopolysaccharide
sulfur compound catabolic process
ear morphogenesis
response to molecule of bacterial origin
cellular response to oxygen-containing compound
Persistently expressed
extracellular matrix organization
collagen fibril organization
antigen processing and presentation of peptide antigen via MHC class
antigen processing and presentation of exogenous peptide antigen via MHC class I, TAP-independent
protein complex subunit organization
-Log10 (P-value)
e
Temporarily downregulated
Temporarily upregulated
Persistently expressed
Transient reprogramming
Complete reprogramming
Mean Log2 RPM
DNA methylation (%)
Fibroblast
Transient reprogramming intermediate
Transiently reprogrammed
iPSC
f
Enhancers of downregulated genes
Enhancers of upregulated genes
Enhancers of persistent genes
Group
Fibroblast
Intermediate stage
Transiently reprogrammed
iPSC
DNA methylation level

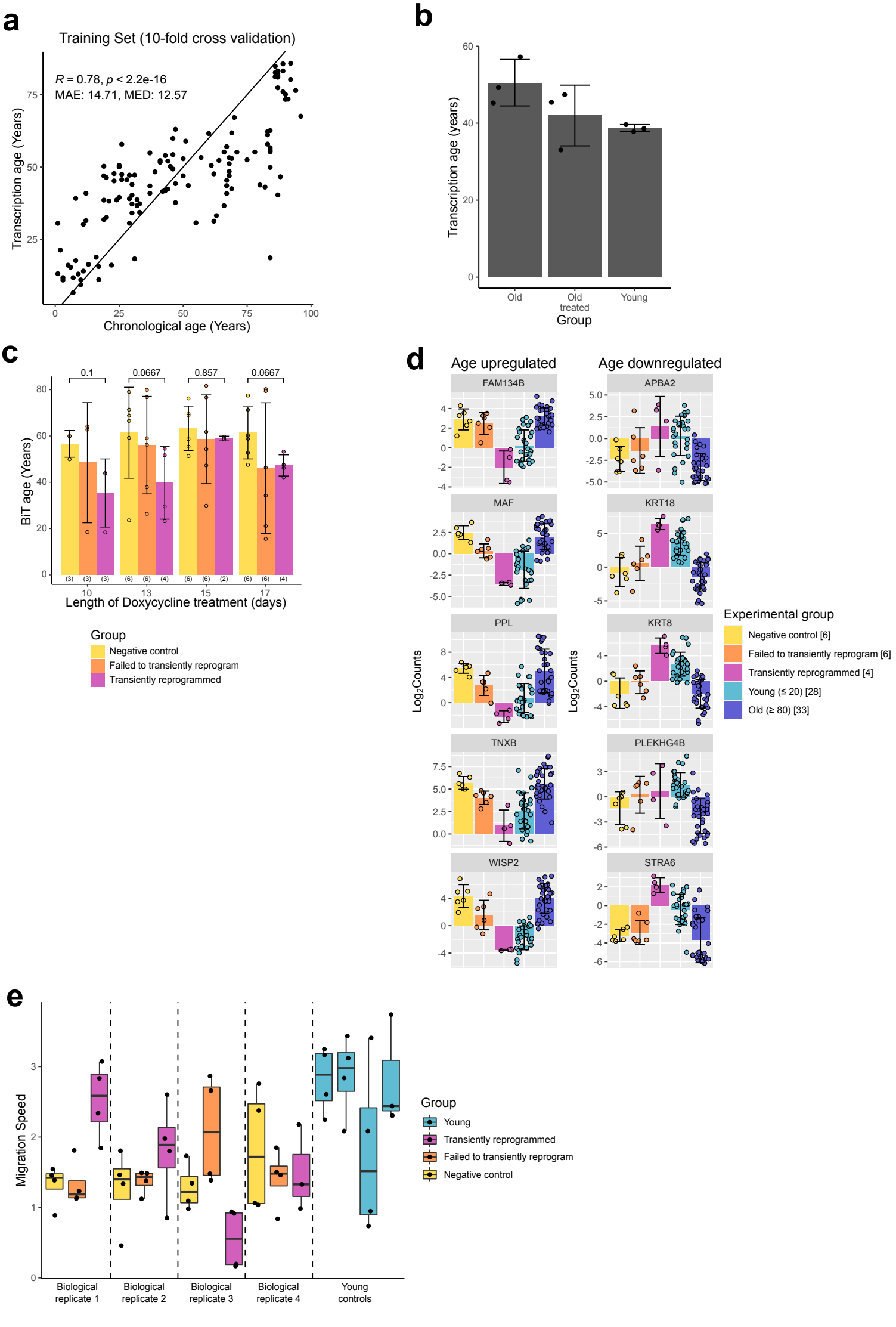
a
Training Set (10-fold cross validation)
R = 0.78, p < 2.2e-16
MAE: 14.71, MED: 12.57
Transcription age (Years)
Chronological age (Years)
b
Transcription age (years)
Old
Old treated
Young
Group
c
0.1
0.0667
0.857
0.0667
BiT age (Years)
Length of Doxycycline treatment (days)
Group
Negative control
Failed to transiently reprogram
Transiently reprogrammed
d
Age upregulated
Age downregulated
FAM134B
APBA2
MAF
KRT18
PPL
KRT8
TNXB
PLEKHG4B
WISP2
STRA6
Log2Counts
Experimental group
Negative control [6]
Failed to transiently reprogram [6]
Transiently reprogrammed [4]
Young (≤ 20) [28]
Old (≥ 80) [33]
e
Migration Speed
Biological replicate 1
Biological replicate 2
Biological replicate 3
Biological replicate 4
Young controls
Group
Young
Transiently reprogrammed
Failed to transiently reprogram
Negative control

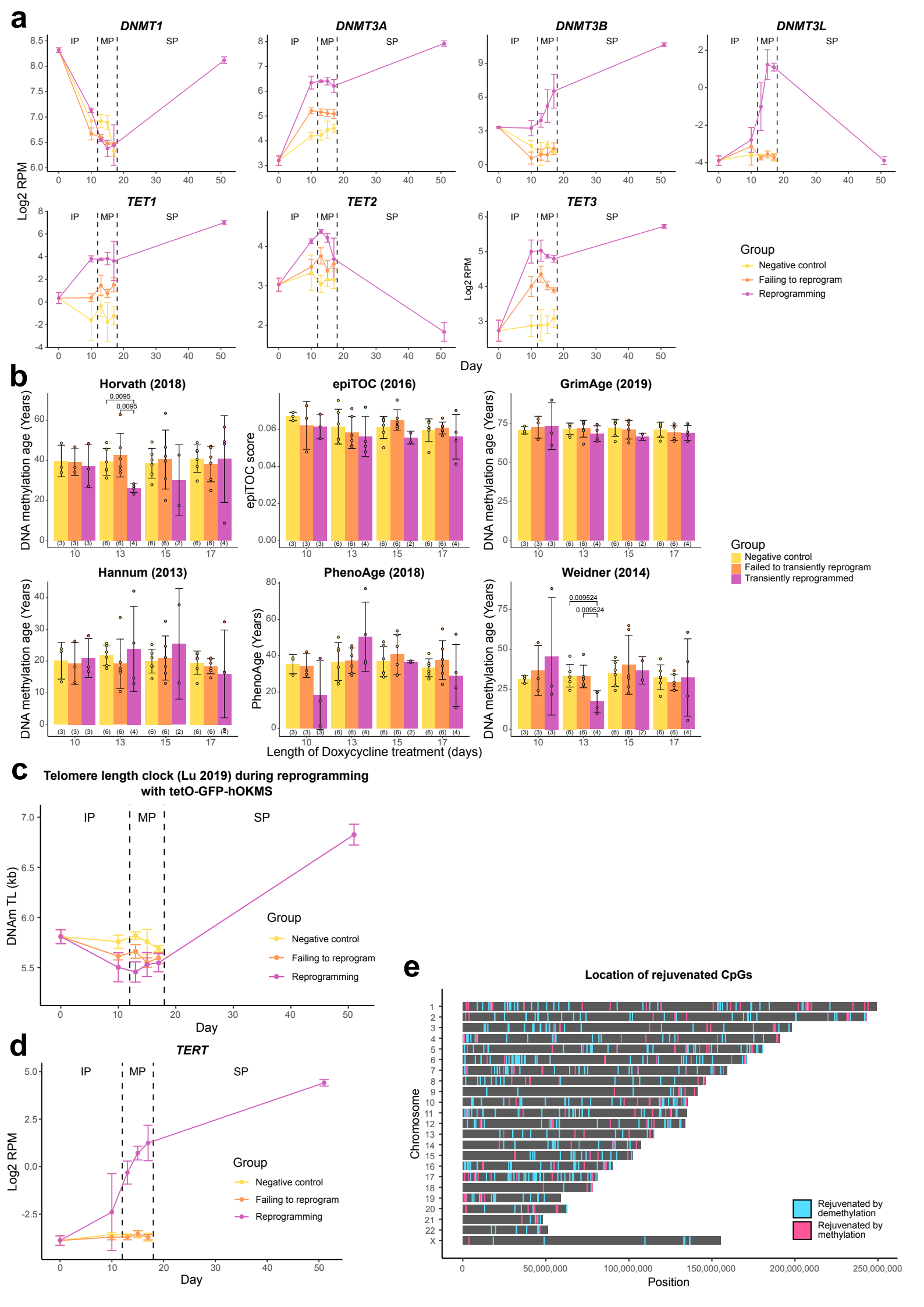
a
DNMT1
DNMT3A
DNMT3B
DNMT3L
TET1
TET2
TET3
IP
MP
SP
Log2 RPM
Day
Group
Negative control
Failing to reprogram
Reprogramming
b
Horvath (2018)
epiTOC (2016)
GrimAge (2019)
Hannum (2013)
PhenoAge (2018)
Weidner (2014)
DNA methylation age (Years)
epiTOC score
PhenoAge (Years)
0.0095
0.009524
Length of Doxycycline treatment (days)
Group
Negative control
Failed to transiently reprogram
Transiently reprogrammed
c
Telomere length clock (Lu 2019) during reprogramming with tetO-GFP-hOKMS
DNAm TL (kb)
Day
Group
Negative control
Failing to reprogram
Reprogramming
d
TERT
Log2 RPM
Day
e
Location of rejuvenated CpGs
Chromosome
Position
Rejuvenated by demethylation
Rejuvenated by methylation